

Cell Host & Microbe

Co-transmission of related parasite lineages shapes within-host parasite diversity --Manuscript Draft--

Manuscript Number:	CELL-HOST-MICROBE-D-19-00301R3
Full Title:	Co-transmission of related parasite lineages shapes within-host parasite diversity
Article Type:	Research Article
Keywords:	Malaria; Transmission; Genomics; Genetics; Single Cell Sequencing
Corresponding Author:	Ian H. Cheeseman Texas Biomedical Research Institute San Antonio, UNITED STATES
First Author:	Standwell C Nkhoma
Order of Authors:	Standwell C Nkhoma Simon G Trevino Karla M Gorena Shalini Nair Stanley Khoswe Catherine Jett Roy Garcia Benjamin Daniel Aliou Dia Dianne J Terlouw Stephan A Ward Timothy JC Anderson Ian H. Cheeseman
Abstract:	<p>Malaria patients frequently carry one or more clonal lineage of the parasite, <i>Plasmodium falciparum</i>. In regions of high transmission, we might expect component parasites within complex infections to be unrelated as a result of parasite inoculations from different mosquitos. This project was designed to directly test this prediction. We generated 485 near-complete single-cell genome sequences isolated from fifteen <i>P. falciparum</i> patients from Chikhwawa, Malawi, an area of intense malaria transmission. Matched single-cell and bulk genomic analyses revealed that patients harbored up to seventeen unique lineages. Current statistical approaches were unable to accurately reconstruct infection composition from bulk sequence data. Surprisingly, our analysis demonstrated that parasite lineages within infections tend to be related, suggesting that superinfection by repeated mosquito bites is rarer than co-transmission of parasites from a single mosquito. Our single-cell analysis indicates strong barriers to establishment of secondary infections, providing new insights into the biology and transmission of malaria.</p>
Suggested Reviewers:	<p>Daniel Hartl, Ph.D Professor, Harvard dhartl@oeb.harvard.edu Prof. Hartl is a population geneticist who has worked extensively on malaria parasite genetics. He has previously published on intrahost relatedness in malaria infections.</p> <p>Dyann Wirth, Ph.D. Professor, Harvard dfwirth@hsph.harvard.edu Prof. Wirth is a malaria parasite geneticist who has worked extensive on malaria parasite population structure, drug resistance and natural selection in malaria parasite populations.</p>

	<p>Christopher Newbold, Ph.D. Professir, University of Oxford chris.newbold@imm.ox.ac.uk Prof. Newbold has worked extensively on parasite genomics and has spearheaded projects on natural variation in malaria parasite populations.</p>
	<p>Photini Sinnis, MD Professor, Johns Hopkins School of Public Health psinnis1@jhu.edu Prof. Sinnis has worked extensively on bottlenecks in transmission throughout the malaria parasite lifecycle. She has used mathematical modelling, cell biology, genetics and field studies to achieve this.</p>
	<p>Sarah Tishkoff, Ph.D. Professor, University of Pennsylvania tishkoff@penmedicine.upenn.edu Prof. Tishkoff is a human geneticist who has often worked on understanding the impact of malaria infection on the human genome.</p>
	<p>Jane Carlton, Ph.D. Professor, New York Univeristy jane.carlton@nyu.edu Prof. Carlton has pioneered population genomics in the malaria parasite Plasmodium vivax. She has been the driving force behind the generation of genome references for multiple malaria parasite species.</p>
<p>Opposed Reviewers:</p>	



Department of Genetics

*Ian H. Cheeseman, Ph.D.*October 10th, 2019

Tel: 210 258 9834

Email: ianc@txbiomedgenetics.org

To the Editors:

Research Article submission: “Co-transmission of related parasite lineages shapes within-host parasite diversity”

We submit for your interest a revised version of our manuscript. We feel we have comprehensively addressed all comments from the reviewers and have considerably strengthened our manuscript. Following comments from Reviewer Two we have also altered the title from “Single cell genomic dissection of complex African malaria infections indicate strong barriers to reinfection” to “Co-transmission of related parasite lineages shapes within-host parasite diversity”.

Malaria infections often contain multiple, genetically distinct parasites. Genetically distinct parasites co-infect an individual through two routes, superinfection, where an individual is bitten by two infected mosquitoes bearing distinct parasites, or co-transmission, where a single mosquito inoculates an individual with multiple parasite genotypes. As sexual recombination between parasite genotypes occurs in the mosquito midgut these two processes give rise to drastically different patterns of within-host variation, and influence the evolution of several biomedically important traits including parasite virulence, antimalarial drug resistance and malaria transmission. Genome sequencing of parasites from malaria infections is commonly used to understand the complexity of infection, but is unable to infer the numbers of clones present or determine the relatedness among parasites within a single host severely limiting the interpretations which can be made.

In the submitted manuscript we use single cell sequencing to understand superinfection and co-transmission in malaria infections. By implementing a highly optimized protocol (Trevino et al, *Genome Biology and Evolution*, 2017) we are able to generate near-complete capture of single parasite genomes. We use this approach to generate the most comprehensive portrait of within-host genetic variation to date, producing ~450 complete single cell genome sequences from across 15 infections from a region of intense malaria transmission.

Surprisingly, we find that superinfection to be rare compared to co-transmission, with most complex infections composed of multiple recently related lineages. These lineages persist across multiple mosquito transmission cycles, with substantial genetic variation maintained during each mosquito bottleneck. Our results strongly suggest that there are barriers that prevent superinfection of malaria infected patients.

These data provide a gold standard for the development of statistical tools for robust deconvolution of malaria infections using bulk sequence data. As we push for malaria elimination it will be crucial for us to understand how genetic variation is maintained in the

Mail: P.O. Box 760549, San Antonio, TX 78245-0549
Shipping: 7620 NW Loop 410, San Antonio, TX 78227-5301
Telephone: 210.258.9834

Website: www.TxBiomed.org
Email: ianc@TxBiomed.org
FAX: 210.258.9131

face of aggressive control and elimination efforts. Our study adds critical depth to our understanding of how within host genetic variation is generated and maintained in areas of intense malaria transmission.

Sincerely,

A handwritten signature in black ink, appearing to read "Ian Cheeseman", with a horizontal line extending to the right from the end of the signature.

Ian Cheeseman, Ph.D.
Milton S. & Geraldine M. Goldstein Young Scientist
Assistant Scientist
Program Lead Host Pathogen Interactions

Dear Dr Lim,

We thank you and the two reviewers for the careful review of our manuscript. The comments were indeed clear and constructive, and have improved the manuscript.

We are mortified that a substandard version of the supplementary material was uploaded for the prior submission. As we described in our previous response there had been a concerted effort to improve the readability of this supplement, and we apologize for wasting time.

In addition, there were errors caught by the reviewers in the submission which we cannot attribute to this oversight. We have corrected these in a substantially revised manuscript. We feel that the comments raised have improved our manuscript and we hope that the revised version is suitable for publication in *Cell Host and Microbe*. We have responded below to each comment and underlined our response.

Dear Ian,

I am enclosing the comments that the reviewers made on your paper. Unfortunately, the consensus recommendation is against publication in *Cell Host & Microbe* in its current form. As discussed previously, we have asked both one of the original reviewers as well as a new reviewer with expertise in parasite genomics to evaluate your revised manuscript. The reviewers continue to refer to the potential interest of the topic and the approach, but cite that significant further work would be necessary for the conclusions to be definitive. Given their comments, we feel that it would be premature to proceed further with the manuscript based on the current presentation. Although we would not necessarily rule out resubmission of a revised manuscript that addresses the reviewers' concerns, it seems that substantial further work, detailed clarification and presentation would be required to achieve this aim. I should also mention that you will not be able to submit a revised version of this manuscript in EM without contacting me first to reactivate the file.

I am sorry that the outcome for this manuscript is not more positive. I hope, however, that the reviewers' comments are clear and constructive.

If you decide not to revise the paper for *Cell Host & Microbe*, you may want to consider transferring the paper to another Cell Press journal. If you are interested in having your paper considered at another Cell Press journal on the basis of these reviews, please contact the editor of the relevant journal directly and I would be glad to assist in transferring the files/information related to your paper. In particular, you may want to consider *Cell Reports* the newest sister journal at Cell Press (<http://www.cell.com/cell-reports/home>).

Best wishes,

Caeul Lim, Ph.D.
Scientific Editor, *Cell Host & Microbe*

Reviewers' Comments:

Reviewer #1: The author provide a revised manuscript in which they describe single cell sequencing of clones from a variety of different *P. falciparum* infections. The revised manuscript is more accessible to a broader audience and the authors have addressed a number of the reviewers' criticisms. However, some of the concerns about the supplementary data have not been addressed—in particular the concern that supplemental figures are illegible remains true. In addition, with this revision, the authors have uploaded a supplement which is apparently full of errors (e.g. missing figures) and which prevents a thorough review. Thus, the comments below are not a full assessment of the manuscript, which cannot be provided given the numerous mislabeled and missing figures.

We are disappointed to have uploaded incorrect supplementary files. This was done in error, and we deeply apologize. We have taken this opportunity to comprehensively review our supplement, figures and legends. We have pushed for greater legibility across the document. These changes include:

- **Detail added to the legend of Supplementary Figures 1,2,4-12**
- **Increased size and legibility of Supplementary Figures 1,5,6,9 & 10**
- **Inclusion of Supplementary Figures 1, 3, 5, 6 & 11 in the main supplement, as well as Supplementary Figure 12 (originally mistakenly described as Figure S8 in the text)**
- **Expansion of Supplementary Figure 8 to include bulk sequencing data**
- **Replacement of Supplementary Figure 7 with two new figures to support the identification of tetrads**

The authors write, "ERSA estimates relatedness between individuals from distribution of IBD tract lengths (Figure 5A, B) using individuals assumed to be unrelated from the same population as a reference. We see a spectrum of relationships within each infection (Figure 5C, Figure S6). It is not clear if the ERSA relationship is in Figure 5 as the legend to Figure 5 does not mention this.

We have corrected this is the revised manuscript. We had updated Figure 5 in the previously uploaded text, but not the stand-alone figure. Both are now in agreement.

Figure S5 and S6 appear to be missing.

Our updated supplement has been revised to include these figures.

The authors write "As seen in previous studies on *P. falciparum* genetic crosses (Jiang et al., 2011) chromosome length and crossover count were correlated ($r_{2344} = 0.8$, $p = 0.0005$, Pearson's correlation, Figure S8)." However, Figure S8 appears to show an IGV screenshot.

We have corrected this error, the figure is now included in the supplement.

Figure S8—two reads does not provide much confidence that the mitochondrial reads are real. Would need to see more data. I cannot assess the quality based on what is provided for review.

We agree with this statement. In our original manuscript we had sought to capture our uncertainty about this site. Line 370-371 “These may have arisen as *de novo* mutations during the current infection, or be artifacts of the WGA and genome sequencing pipeline”. We have further clarified this Line 317-322 “However, as these may have arisen as *de novo* mutations during the current infection, or be artifacts of the WGA and genome sequencing pipeline we excluded this site from further analysis” and added additional detail to the supplementary figure supporting this statement. We do not believe the site supported by 2 reads in Cell 4 is the *de novo* mutation. Cell 4 shares complete identity to the dominant haplotype in the infection. We have included the bulk sample to the IGV plot supporting this in supplementary figures 7, and show complete mitochondrial genotypes in supplementary figure 8. We believe the *de novo* mutation we refer to is present in cells 9 and 22 and supported by 31 and 28 reads respectively. We thank the reviewer for the chance to clarify this point.

Overall the discussion of mitochondrial inheritance is poorly written and it is difficult to follow. Sparse figure legends do not help. The authors reference Figure 5D, which does not apparently exist.

We thank the review for these comments, we have rewritten much of this section to provide clarity and provided an updated version of Figure 5. Briefly, we show that parasites with identical genotypes in their nuclear genome also have identical genotypes in their mitochondrial genome. We have moved this section to improve the flow and substantially rewritten it changing to:

“Mitochondrial inheritance within individual infections

Mitochondria are inherited maternally during malaria parasite meiosis and therefore allow the identification of parasites which share a maternal lineage within infections. We found 93 SNPs in the mitochondrial DNA which varied within our dataset. Across all 498 parasites we were able to capture the genotype of 79.1% (36,645/46,314) of these 93 sites. We expect parasites which are identical across their nuclear chromosomes to also be identical across their mitochondrial genome. We find this to be the case. Within individual hosts, parasites which shared 100% of their genome IBD also shared 100% of their mitochondrial genome sequence. Across the 498 genome sequences for which we had reliable estimates of genome-wide IBD and mitochondrial genotypes there were only 2 of a possible 36,645 sites (0.0055%) where the mitochondrial genotype varied within a group of parasites which were 100% IBD. These arise at position 1,692 in cells 9 and 22 of infection MAL24. Visual inspection of these sites (Figure S7) and the presence of the reads supporting both genotypes in the bulk genome sequence supports these being genuine. However, as these may have arisen as *de novo* mutations during the current infection, or be artifacts of the WGA and genome sequencing pipeline we excluded this site from further analysis.

We identified a total of 20 unique mitochondrial haplotypes across the entire dataset (Figure S8 and Figure S9). We counted the number of mitochondrial haplotypes present in each infection (Figure 5D). This showed 9 infections contained a single mitochondrial haplotype, 3 infections contained 2 haplotypes, 1 infection contained 3 haplotypes, and 2 infections contained 4 haplotypes. All monoclonal infections contained a single mitochondrial haplotype, as did 4/10 (40%) polyclonal infections. Within polyclonal infections distinct mitochondrial haplotypes were observed between very close relatives (sharing >60% of their genomes IBD) supporting the retention of diversity we observe in the face of recurrent inbreeding. As mitochondria are uniparentally inherited the presence of multiple mitochondrial haplotypes across related parasites from within the same infection demonstrates multiple oocysts within a mosquito are responsible for initiating an infection. We tested if a higher level of shared pair-wise IBD is a predictor of sharing a mitochondrial haplotypes between two parasites. After excluding clonally identical parasites we estimate a 10% increase in IBD shared between parasites from the same infections increasing the odds of sharing a mitochondrial genotype by a factor of 10.082 ($p=5.25 \times 10^{-8}$, logistic regression).”

Figure S9 and S10 are still illegible. What is UPGMA? What are the axes? "Height" is upside down.

We have increased the font size, provided a more appropriate label for the axis and greater detail in the figure legends for these two plots. In addition, they are now correctly labelled as Figures S10 and S11.

Reviewer #2: This is an intriguing and important manuscript which uses single cell genomics to carefully define the complexity of infection in Plasmodium falciparum clinical isolates. It is well established that individuals in high transmission regions are often infected with multiple different P. falciparum haplotypes, but exactly how many, and how they are related to each other, has been difficult to determine. The approach used, single cell genome sequencing, is cutting edge, because while scRNAseq is becoming increasingly applied to Plasmodium research, single cell genome sequencing is more challenging to generate because there is only a single copy of the genome in each cell, rather than the multiple copies of most RNA species. This is therefore an important question using novel technologies. Quality control of the single cell data is clearly key, but appears to be rigorous - there is little evidence of contaminating DNA from other sources, and samples with mixed calls, which could indicate the presence of two cells in the source material instead of one, are eliminated. The central findings are really two fold - one technical, that single cell sequencing can be used to deconvolute mixed infections, and one biological, and that individuals are more often infected with related parasite genotypes than might be expected. The former seems clearly proven, with some technical clarification required as noted below. The latter is also clear and important, although there is some confusion in the way the methodologies are applied and inferences derived, and the title rather overstates the generalisability of the findings. Suggested areas for clarification are enumerated below:

Major issues

1. Amplification bias. A key question is obviously one of bias in the single cell sequence data. Whole Genome Amplification is used to amplify the material, but why WGA and not selective

WGA which might give more even coverage across the genome? No details about the WGA method are provided in line 548, and depending on the method, the worry is that it will result in bias towards some (presumably slightly less AT-rich) regions of the genome. Is there evidence of this? One would guess so, based on the fact that only 60,002 SNPs were scored, and 10,997 used for downstream analysis, which is a relatively low number for *P. falciparum* genomic analysis, but no details are given. Given that the same SNPs are used in all samples, it doesn't necessarily invalidate the interpretation, but much more clarity about the single cell sequencing methodology and limitations thereof is required.

We thanks the reviewer for these comments and the opportunity to provide greater detail to our approach. We have published two previous papers, Nair et al, Genome Research, 2012 and Trevino et al, Genome Biology and Evolution, 2017 where we have included extensive details about the development of the WGA protocol we implement here. We appreciate that these were not appropriately cited in the manuscript. This has been corrected, and we have added some additional detail to this section at lines 530-532, and 579-586 of the revised manuscript.

In short, we have opted for WGA as it outperforms sWGA. In a recent paper (Oyola, Ariani et al, Malaria Journal 2016) using an input of 40 parasites less than 50% of the genome was captured. Selective WGA, even with an excess of parasite templates, appears to plateau at 85% of the genome covered. When limiting samples to the same criteria as that paper (libraries with at least 20M reads) our approach captures 95% of the genome with 5 or more reads, similar to our published estimates (Trevino et al, Genome Biology and Evolution, 2017). We have previously shown (Nair et al, Genome Research, 2012) that any bias from this approach is stochastic, rather than deterministic and not correlated with AT content. As we have published multiple papers describing the methodology applied here we opt to refer readers to these more comprehensive analysis rather than include further details here.

There was an additional concern that we had scored a low number of mutations for a malaria genomic survey. We agree there was insufficient detail included to appropriately judge how comparable our data is to other malaria genome sequencing efforts. We have added further details on our SNP calling pipeline, and variant filtering to highlight that the numbers here are not low, but are conservatively called. Notably, we include a larger subset of variant sites (~175K SNPs, Line 143) used during initial quality control of the data. To investigate this further we compared our results to SNP calls from the Pf3K project a large, well curated dataset limiting our comparison to chromosome 1 and the 317 samples in Chikhwawa, Malawi present in the Pf3K data. Our genotyping pipeline and filtering was based upon the Pf3K methods and correspondingly we find very similar numbers of common sites (for MAF>0.05: 1,021 in our data and 1,102 in Pf3K and for MAF>0.01: 2,666 in our data and 2,791 in Pf3K). Due to the larger sampling Pf3K has a larger amount of variants when no minor allele frequency is applied (2,666 in our data and 8,652 in Pf3K). In short, we believe the SNP calling in our data is comparable with contemporary approaches.

2. Correlation between number of haplotypes called by bulk sequencing of single cell data. Figure 2C suggests that there is considerable disconnect between the calls of complexity made from bulk and single cell sequence data, with several infections on the left hand side of the x axis having 1-3 haplotypes identified from single cell rarefaction, despite having lower Fws scores. Purely visually, this doesn't seem in keeping with Figure 3A, where the correlation seems much higher. Is this because the "effective number of haplotypes" estimated from single cell data used in Figure 3 is different from the number of haplotypes estimated from the same data in Figure 1C? If these are indeed different methods (which is what I guess is happening), it does not come across clearly at all in the manuscript. Clearer explanation and pros/cons of each method would seem useful to include. On a related note, in Figure 3A, the outliers all lie under the trend line suggest that either Fws is overestimating complexity, or single cell is underestimating. That is the opposite of what I would expect, given the difficulty of detecting strains present in minor abundance. Is there an explanation for this? This comment speaks to a general issue of the paper - multiple different methods and computational tools are used somewhat interchangeably, without clear rationale or explanation in some places. For the non-expert reader, it will still be difficult to follow, and more clarity is required.

We thank the reviewer for the ability to clarify this important point in our manuscript. There are multiple distinct estimates of the number of haplotypes present in an infection presented here. The first, FWS, captures unfixed sites and is highly effective at capturing clonal vs. non-clonal. Beyond this there is no expectation that a specific FWS value will capture "complexity" in a discrete way. There are two estimates of the actual number of haplotypes, one from DEploid and inferred from bulk sequencing, the other by single cell sequencing. These measure the same thing, though do not agree perfectly in this analysis. In an effort to compare across all measures the effective number of haplotypes (introduced as part of DEploid by Zhu et al) normalizes the number of haplotypes by their abundance. These measures are concordant as they all account for abundance. We have added additional detail on each approach in lines 225-229 to address the lack of clarity.

3. In Figure 4, are all the bulk sequencing squares coloured using the same code that the single cell sequencing squares are? A few clusters (the colour code is hard to follow, see below) seems to lack a bulk sample - how is this possible? And is it useful to include all the bulk samples in this figure, given that most didn't have single cell data called, and so simply sit at the upper right of the figure?

We have included an updated version we hope will be clearer for readers. All infections with single cell data also have a bulk sequence. For the figure there are occasions where the bulk and single cell are identical, and this has obscured the bulk dot. We have made these more prominent in the revised figure. We feel it is important to include the data which does not fall within the network. The alternative would suggest far greater connectivity is present in the general population than we detect. We have wrestled with the color schemes to attempt to improve clarity. This is not trivial with a large number of infections.

4. Possible causes of higher than expected level of relatedness observed in complex infections. The data in Figure 5 is compelling, and novel. A key question is how generalisable it is - whether there is something unusual or unique about this sample collection/study site that could explain the finding. While expanding to more locations is clearly out of scope of this manuscript, some consideration of this issue in the Discussion might be useful. For example, if the infections were from a region where transmission was high by highly fragmented, with pockets of high transfection surrounded by arid, low transmission regions, then this kind of pattern might be more expected. If transmission is more uniform in the area, then the findings are more surprising and significant. Before making a general case that complex infections are frequently formed from related parasites, it is critical to state the epidemiological context and possible confounders.

We agree that the sample size possible in this work does limit how generalizable the findings are. We have included a more detailed discussion of the context in lines 417-425.

“In this work we have generated a detailed picture of within-host genetic variation across fifteen malaria patients. While this is a modest number of infections, these findings are directly informative about the limits of malaria complexity. We have surveyed a high transmission setting and focused on polyclonal infections. This sampling enriches for infections with the highest likelihood of genetic diversity arising from superinfection rather than co-transmission. In spite of this we find co-transmission to be widespread, and likely underappreciated as a mechanism generating and maintaining genetic diversity in natural malaria populations. There is a pressing need to extend these observations across the range of malaria endemicity to fully capture the transmission network of malaria infections.”

5. Title. I'm not convinced that the manuscript actually shows that there are strong barriers to reinfection. What has been shown is a higher than expected rate of inbreeding. There could be many explanations for this, some epidemiological as noted above, and until repeated in different contexts, I think I would be very hesitant to say anything as definitive as the title implies....

We have now modified the title to “Co-transmission of related parasite lineages shapes within-host parasite diversity” to better convey the key observation from this work

Minor issues

1. Figure 4. Given the colour scheme has multiple relatively similar colours, it's quite hard to translate from the key to individual infections. Given this figure is used to highlight examples of superinfection and cotransmission, alternative labelling is needed - either by indicating more clearly (for example with circles, or arrows) on the figure the examples that are referred to in lines 258-260 (MAL5, 15, 23 and 24), or coming up with a different scheme to label all the infections which doesn't have the same issue of similar colouring...

We thank the reviewer for this suggestion. We agree the suggested scheme improves the ability to understand the figure and have updated the figure.

Typographical errors

1. Line 52 - analyse not analysis?
2. Line 79 - single parasite genotype present presumably refers only to Figure 1A?
3. Line 258 - missing "that"?

Thank you, we have corrected these errors

Co-transmission of related parasite lineages shapes within-host parasite diversity

Standwell C. Nkhoma^{1,2,3,4,*†}, Simon G. Trevino⁴, Karla M. Gorena⁵, Shalini Nair⁴, Stanley Khoswe¹, Catherine Jett⁴, Roy Garcia⁴, Benjamin Daniel⁵, Aliou Dia⁴, Dianne J. Terlouw^{1,2}, Stephen A. Ward², Timothy J.C. Anderson⁴, Ian H. Cheeseman^{4,6,*}

¹Malawi-Liverpool-Wellcome Trust Clinical Research Programme, University of Malawi College of Medicine, Blantyre, Malawi.

²Liverpool School of Tropical Medicine, Liverpool, United Kingdom.

³Wellcome Trust Liverpool Glasgow Centre for Global Health Research, Liverpool, United Kingdom.

⁴Texas Biomedical Research Institute, San Antonio, Texas, United States of America.

⁵University of Texas Health Science Center San Antonio, San Antonio, Texas, United States of America.

⁶Lead Contact

*Correspondence: ianc@txbiomed.org, snkhoma@atcc.org

† Present Address: **Malaria Research and Reference Reagent Resource Center (MR4), BEI Resources, ATCC, Manassas, VA, USA**

SUMMARY

In high transmission regions, we expect parasite lineages within complex malaria infections to be unrelated due to parasite inoculations from different mosquitoes. This project was designed to test this prediction. We generated 485 single-cell genome sequences from fifteen *P. falciparum* malaria patients from Chikhwawa, Malawi, an area of intense transmission. Patients harbored up to seventeen unique parasite lineages. Surprisingly, parasite lineages within infections tend to be closely related, suggesting that superinfection by repeated mosquito bites is rarer than co-transmission of parasites from a single mosquito. Both closely and distantly related parasites comprise an infection, suggesting sequential transmission of complex infections between multiple hosts. We identified tetrads and reconstructed parental haplotypes which revealed the inbred ancestry of infections and non-Mendelian inheritance. Our analysis suggests strong barriers to secondary infection and outbreeding amongst malaria parasites from a high transmission setting, providing unexpected insights into the biology and transmission of malaria.

INTRODUCTION

Malaria remains a major global health problem, with ~400,000 malaria-related deaths in 2015, and over 200 million clinical cases (WHO, 2016) cases. The intensity of malaria transmission is correlated with the complexity of infection (COI), the number of genetically distinct parasites observed within a single infection. Genetically distinct malaria parasites can infect an individual through two routes (Figure 1). A single individual may be bitten by two (or more) infected mosquitoes, each bearing a unique parasite genotype (Figure 1B), or an individual may be bitten by a single mosquito bearing more than one parasite genotype (Figure 1C). Throughout, we refer to these two processes as superinfection and co-transmission respectively. Superinfection of an individual by multiple infectious mosquito bites is often used to explain the high complexity of infection found in high transmission regions (Volkman et al., 2012). Following a bloodmeal, gametocyte stage parasites fuse in the mosquito midgut, and an obligate round of sexual recombination occurs. If only a single parasite genotype is present, all offspring will be identical (Figure 1A, B). When multiple parasite genotypes are present recombinant progeny

51 may arise (Conway et al., 1991, Mu et al., 2005, Nkhoma et al., 2012, Wong et al., 2017, Wong
52 et al., 2018) (Figure 1C). At a population level recombination of parasite genotypes shapes the
53 local decay of linkage disequilibrium and haplotype variation (Mu et al., 2005, Mu et al., 2007,
54 Neafsey et al., 2008).

55
56 The clinical impact of complex infections has been studied in mouse malaria models. Here,
57 interactions between genetically distinct malaria parasites are known to influence the evolution
58 of parasite virulence, antimalarial drug resistance, immunity, gametocyte sex ratios, and malaria
59 transmission (Bell et al., 2006, de Roode et al., 2005, Wargo et al., 2007a, Wargo et al., 2007b,
60 Reece et al., 2008). However, translating these findings to human malaria has been a major
61 challenge. This is due to the paucity of appropriate tools for resolving infection complexity on a
62 large-scale at the level of single parasitized cells: we cannot directly infer the composition of
63 malaria infections by bulk sequencing of infected blood samples. Complex infections confound
64 most traditional genetic analysis, preventing the accurate inference of allele frequencies and
65 even simple genotype-phenotype associations (Nair et al., 2014, Wong et al., 2018). However,
66 powerful new approaches to analyze individual malaria infections are emerging, aided by recent
67 advances in targeted capture of singly-infected erythrocytes from complex mixtures and
68 improved methods for single-cell sequencing (Nair et al., 2014, Trevino et al., 2017), and
69 computational approaches for interpreting infection complexity (Chang et al., 2017, Zhu et al.,
70 2018).

71
72 Using single-cell sequencing and cloning parasites by limiting dilution from a single individual,
73 we previously saw a range of inferred relationships amongst co-infecting parasite haplotypes,
74 including identical clonal lineages, siblings and unrelated individuals (Nair et al., 2014, Nkhoma
75 et al., 2012, Trevino et al., 2017). However, it is unknown to what extent these findings can be
76 generalized across a population. This project was designed to understand the degree to which
77 the genetic diversity of individual infections is driven by superinfection of unrelated strains, or
78 co-transmission of related ones. To do this, we performed whole genome sequencing of bulk
79 infections and single-cell sequencing of parasite-infected cells isolated from malaria patients in
80 Chikhwawa, a high transmission region in Malawi.

81 82 83 **RESULTS**

84 **Infection complexity in bulk sequenced samples**

85 To resolve the within-host population structure of malaria infections, we performed a cross-
86 sectional survey of individuals infected with uncomplicated *P. falciparum* malaria in Chikhwawa,
87 Malawi, an area of high malaria transmission (entomological inoculation rate 183 infectious bites
88 per person per year (Mzilahowa et al., 2012). In this setting, we might expect that patients will
89 contain a mixture of unrelated parasites, resulting from independent mosquito inoculations (i.e.
90 that superinfections will predominate). We performed bulk parasite genome sequencing of 49
91 infections to a median read depth of 31 (interquartile range 20.93-48.37). We estimated the
92 complexity of infection from bulk sequence data using 10,997 unfixed SNP positions with a
93 minor allele frequency (MAF) >0.05 using the F_{WS} statistic (Auburn et al., 2012, Manske et al.,
94 2012) and DEploid (Zhu et al., 2018) (Figure 2a,b, Table S1). F_{WS} grades infections on a
95 continuous scale of complexity where infections with an $F_{WS}>0.95$ are considered clonal and
96 DEploid estimates the number of haplotypes (K) present in sequence data by jointly estimating
97 haplotypes and their abundances. In close agreement with contemporary estimates of within-
98 host diversity (Early et al., 2018) from the same location, 22 of 49 infections (44.9%) were
99 considered clonal by F_{WS} . The within-host allele frequency (WHAF) captured from deep
100 sequencing can be used to infer the presence of related parasites (Pearson et al., 2016). The
101 patterns of unfixed mutations in the remaining 27 infections suggest a simple model of

102 superinfection is insufficient to universally capture all patterns of within-host relatedness (Data
103 S1). Across the genome the WHAF in superinfected patients cluster around three values: fixed
104 to the reference allele; fixed to the alternative allele; or at an intermediate frequency determined
105 by the proportion of the two strains. Analysis of bulk sequencing data could not definitively
106 resolve superinfection and co-transmission, so we selected 15 infections across the range of
107 F_{WS} and inferred K (the number of haplotypes present) for single-cell sequencing, using a
108 recently optimized method capable of near-complete genome capture (Trevino et al., 2017). The
109 malaria parasite undergoes 4-5 rounds of DNA replication within a single-cell producing
110 segmented schizont stage parasites with an average of 16 genome copies (Reilly et al., 2007).
111 We isolate individual schizonts by Fluorescence Activated Cell Sorting (FACS), followed by
112 whole genome amplification (WGA) under highly sterile conditions before sequencing the
113 amplified product.

114 115 **Single-cell sequencing of malaria parasites**

116 In total we sequenced the genomes of 485 single-cells subjected to WGA (437 unique to this
117 study), 49 bulk infections and 24 clones isolated from a single patient by limiting dilution
118 (Nkhoma et al., 2012, Rosario, 1981). Prior to genotype filtering we scored 175,543 biallelic
119 SNPs with a $VQSLOD > 0$ across the 558 genome sequences. The highly repetitive and AT-rich
120 *P. falciparum* genome (Gardner et al., 2002) presents unique challenges with generating an
121 accurate picture of the variation present in a single-cell. We were particularly concerned with
122 capture of DNA from more than one genetic background during the single-cell sequencing
123 protocol and implemented stringent quality checks. Using sequencing data from the 24 clones
124 we estimated the threshold for identifying single-cell sequences where there was potential
125 contamination from exogenous DNA at 1% of mixed base calls. The sequences from the cloned
126 lines were integrated into the single-cell dataset for downstream analysis. After excluding low
127 coverage libraries ($< 75,000$ calls, $n=23$) and sequences with $> 1\%$ mixed base calls ($n=38$) 424
128 single-cell sequences remained. After including 23 of the sequences from *ex vivo* expanded
129 clones there were 13-45 sequences per infection (mean 29.9 sequences; Figure S1). The
130 number of haplotypes per sample attempted was estimated by rarefaction analysis (described
131 below).
132

133 After quality control we retained 60,002 SNPs scored in at least 90% of the 496 sequences,
134 10,997 of which had a $MAF > 0.05$ across the 49 bulk sequenced infections. As the 10,997 SNPs
135 were ascertained from population data which did not undergo whole genome amplification this
136 category of SNPs are unlikely to be artifacts from the MDA reaction, nor mutations arising
137 during the course of an infection. Across our dataset parasites classified as clonally identical
138 were identical at 99.97% of the original 60,002 sites, equivalent to a genome-wide error-rate of
139 1.2×10^{-6} mutations per basepair per cell, suggesting our approach is comparable (or superior) to
140 leading single-cell sequencing methods (Leung et al., 2015, Hou et al., 2013, Lu et al., 2012).
141 As an initial characterization of our data we estimated the genetic diversity in each infection
142 from the number of unfixed sites from read pileups in bulk sequencing or across called
143 genotypes in single-cell sequencing. For paired bulk/single-cell data from the same infection a
144 mean of 1.6 fold (range 0.7-9.1 fold) more polymorphic sites were discovered by single-cell
145 sequencing than by bulk sequencing (Figure S2). This is likely due to the limits in discovery of
146 very low frequency SNPs by bulk sequencing. By subsampling our single-cell data we saw
147 diminishing returns from sequencing additional cells, with 90% of the observed polymorphic
148 sites captured by sampling a mean of 21.6 cells (range 7-43, Figure S2).
149

150 **Haplotypic diversity of malaria infections**

151 An important goal in malaria genomics is estimating the number of unique haplotypes (or
152 complexity of infection) within an infection (Volkman et al., 2012). We estimated the number of

153 unique haplotypes directly from the single-cell data. To exclude potential confounding of *de*
154 *novo* mutation and sequencing error, we restricted analysis to 10,997 conservatively called sites
155 with a MAF >0.05 in the 49 bulk sequenced infections. We estimated the number of unique
156 haplotypes per infection by collapsing haplotypes from the same infection that were different at
157 <1% of sites. For each infection, we applied individual-based rarefaction to the haplotype
158 abundances and sequenced additional single genomes until a plateau in the rarefaction curve
159 was reached (Figure S2). Using this approach, between 1 and 17 haplotypes were observed in
160 each infection (Figure 1C, Table S1). Rarefaction of haplotype abundance suggested we had
161 captured all haplotypes present in 14/15 infections. For these 14 samples the number of
162 haplotypes captured was within the 95% confidence interval of the Chao I estimator. One
163 infection (MAL15) showed exceptionally high diversity with 17 of an estimated 30.21 (95%
164 CI=19.7-81.7) haplotypes detected. Two infections (MAL37 and MAL33) show a single
165 haplotype from single-cell sequencing, although F_{WS} scores <0.95 and patterns of segregating
166 sites suggest we have incompletely captured all haplotypes (Data S1). Sequencing more cells
167 did not capture additional haplotypes.

169 **Inference of infection composition from bulk sequences**

170 There has been a concerted effort to develop statistical methods for inferring the parasite
171 haplotypes within complex infections using information from bulk sequence data (Chang et al.,
172 2017, Zhu et al., 2018). Such methods aim to phase haplotype data from complex mixtures,
173 extending the methods used to infer haplotypes from diploid genotypes. Our single-cell
174 resolution data from natural infections provides “gold standard” data for comparison with
175 inferences. We found a strong correlation between the effective number of haplotypes (Zhu et
176 al., 2018) observed by single-cell sequencing and the effective K from DEploid (Pearson’s
177 $r^2=0.61$) and F_{WS} (Pearson’s $r^2=-0.51$, Figure 3A,B). The effective K and effective number of
178 haplotypes normalizes the absolute haplotype number by the abundance of each haplotype and
179 are distinct from the number of haplotypes presented in Figure 2. As within-host abundance is
180 accounted for in these measures (and in F_{WS}) it is not surprising these agree more closely than
181 when comparing absolute haplotype number or Inferred K. However, while DEploid performed
182 well in determining the predominant haplotype present within infections, it was unable to
183 accurately determine the additional haplotypes present within infections (Figure 3C). The poor
184 performance most likely stems from the assumption that haplotypes found within infections are
185 unrelated. We suggest that incorporating relatedness into these models may improve
186 performance of these inference methods. Importantly, our data provide a suitable dataset for
187 optimizing and improving these statistical models.

189 **Recent ancestry of individual infections**

190 The size of chromosomal blocks that are shared identical-by-descent (IBD) between infections
191 provides a metric for assessing parasite relatedness: recent relatives share large blocks, while
192 in distant relatives these blocks are smaller because they have been broken up by
193 recombination events. As recombination occurs in the mosquito (Figure 1) related parasites are
194 likely to have arisen from a single mosquito bite and have been co-transmitted. To better
195 characterize levels of relatedness within infections we identified blocks of chromosomes shared
196 IBD between all paired sequences using a hidden Markov model (Schaffner et al., 2018). IBD
197 sharing between clonal bulk sequenced infections was rare, with a mean of 0.73 blocks shared
198 between infections (range 0-5), encompassing a mean of 88.5kb (range 3.8-342.7kb) of each
199 genome, with a mean block length of 50.8kb (range 3.8-142.4kb). In contrast, within infections
200 parasites shared a mean of 13.0 (range 0-30) IBD blocks between parasite genomes,
201 encompassing a mean of 16,334.2kb (range 3.1-20,577.0kb) of each genome, with a mean
202 shared block length of 1,143.6kb (range 3.1-1469.8kb). As we limit inference of IBD to the ‘core’
203 genome (Miles et al., 2016) identical parasites share 20,577kb of their genomes IBD in 14

204 blocks (one per chromosome). The presence of IBD sharing between individuals supports
205 recent shared ancestry. For 10/15 of the infections there was at least one block of IBD shared in
206 all pairwise comparisons. As our filtering of IBD blocks was limited to >2.5cM we are limited to
207 inference of relatedness over the last 25 generations (~6 years (Henden et al., 2018)).
208

209 Recent studies have highlighted the power of IBD networks to capture the structure of a parasite
210 population (Henden et al., 2018). We built a network of pairwise shared IBD, creating links
211 between parasites with >15% of their genomes shared IBD (Figure 4, Data S2). This revealed
212 close connectivity between parasites from the same infection, with much sparser connectivity
213 between parasites from different infections. We observed subdivision within individual infections.
214 For instance, MAL5 and MAL24 form two clusters of parasites that were connected by the
215 sequence derived from bulk sequencing to one another in agreement with expectations of
216 superinfection. MAL15 and MAL23 show either direct connections or indirect connections
217 (passing through another genotype) between all parasites in agreement with the expectations of
218 co-transmission. Varying the minimum IBD required to connect genomes allowed us to visualize
219 how relatedness subdivides individual infections across a range of IBD sharing (Data S2).
220

221 The distribution of total pairwise shared IBD and the average shared block lengths can be used
222 to infer the relationships between individual genomes (Huff et al., 2011, Li et al., 2014). We
223 inferred the degree of relatedness from our data using the Estimation of Recent Shared
224 Ancestry (ERSA) algorithm. Under this scheme 0 denotes identical clones, 1 denotes parent-
225 sibling, 2 denotes full/half siblings with higher numbers denoting increasingly distant
226 relationships. ERSA estimates relatedness between individuals from distribution of IBD tract
227 lengths (Figure 5A, B, Figure S3) using individuals assumed to be unrelated from the same
228 population as a reference. We see a spectrum of relationships within each infection (Figure 5C).
229 In MAL5 this confirmed the lack of relatedness between the two clusters of parasites,
230 suggesting this infection was the result of a genuine superinfection. However, no other
231 infections can be classified so simply, commonly showing relationships as distant as 4th degree
232 (equivalent to 'first cousins'). Within our data this suggests that it is not uncommon for parasites
233 to be transmitted through two generations (human-mosquito-human-mosquito-human), with up
234 to four generations of co-transmission seen in our data in infection MAL24 and MAL17. In our
235 data we see only a single unambiguous instance of superinfection of two unrelated parasites
236 with no concurrent co-transmission (MAL5). Across the analysis, the genetic diversity of three
237 infections (MAL17, MAL24 and MAL48) appears to be driven by both superinfection of unrelated
238 parasites and co-transmission of related parasites (in addition to MAL5 where only
239 superinfection is suspected).
240

241 **Mitochondrial inheritance within individual infections**

242 Mitochondria are inherited maternally during malaria parasite meiosis and therefore allow the
243 identification of parasites which share a maternal lineage within infections. We found 93 SNPs
244 in the mitochondrial DNA which varied within our dataset. Across all 498 parasites we were able
245 to capture the genotype of 79.1% (36,645/46,314) of these 93 sites. We expect parasites which
246 are identical across their nuclear chromosomes to also be identical across their mitochondrial
247 genome. We find this to be the case. Within individual hosts, parasites which shared 100% of
248 their genome IBD also shared 100% of their mitochondrial genome sequence. Across the 498
249 genome sequences for which we had reliable estimates of genome-wide IBD and mitochondrial
250 genotypes there were only 2 of a possible 36,645 sites (0.0055%) where the mitochondrial
251 genotype varied within a group of parasites which were 100% IBD. These arise at position 1,692
252 in cells 9 and 22 of infection MAL24. Visual inspection of these sites (Figure S4) and the
253 presence of the reads supporting both genotypes in the bulk genome sequence supports these
254 being genuine. However, as these may have arisen as *de novo* mutations during the current

255 infection, or be artifacts of the WGA and genome sequencing pipeline we excluded this site from
256 further analysis.

257
258 We identified a total of 20 unique mitochondrial haplotypes across the entire dataset (Figure S5
259 and Figure S6). We counted the number of mitochondrial haplotypes present in each infection
260 (Figure 5D). This showed 9 infections contained a single mitochondrial haplotype, 3 infections
261 contained 2 haplotypes, 1 infection contained 3 haplotypes, and 2 infections contained 4
262 haplotypes. All monoclonal infections contained a single mitochondrial haplotype, as did 4/10
263 (40%) polyclonal infections. Within polyclonal infections distinct mitochondrial haplotypes were
264 observed between very close relatives (sharing >60% of their genomes IBD) supporting the
265 retention of diversity we observe in the face of recurrent inbreeding. As mitochondria are
266 uniparentally inherited the presence of multiple mitochondrial haplotypes across related
267 parasites from within the same infection demonstrates multiple oocysts within a mosquito are
268 responsible for initiating an infection. We tested if a higher level of shared pair-wise IBD is a
269 predictor of sharing a mitochondrial haplotypes between two parasites. After excluding clonally
270 identical parasites we estimate a 10% increase in IBD shared between parasites from the same
271 infections increasing the odds of sharing a mitochondrial genotype by a factor of 10.082
272 ($p=5.25 \times 10^{-8}$, logistic regression).

273 274 **Identification of meiotic siblings and reconstruction of parental haplotypes**

275 During meiosis a tetrad of four recombinant progeny arise from a single paired set of
276 chromosomes. Genetic characterization of tetrads has enabled precise capture of tracts of gene
277 conversion, cross-overs and non-cross-overs in yeast, mammalian and plant genetics (Cole et
278 al., 2014, Hou et al., 2013, Mancera et al., 2011, Li et al., 2015). Identifying progeny which
279 came from the same tetrad, rather than simply sharing the same parents, allows us to estimate
280 the number of ookinetes giving rise to an infection. As meiotic siblings share reciprocal
281 recombination breakpoints, it also enables a fine-scale measurement of gene conversion and
282 non-Mendelian inheritance in natural infections. Chance identification of potential meiotic
283 siblings in low transmission regions (Dharia et al., 2010) and *P. vivax* (Bright et al., 2014) has
284 suggested that tetrad analysis may be feasible. We identified potential members of tetrads as
285 those sharing the same mitochondrial genotype with a coefficient of relatedness of 1, which
286 would contain half-sibs, full-siblings, and meiotic siblings. For each group we inferred the
287 parental haplotypes and recombination breakpoints using Hapi (Li et al., 2018). Following this
288 we filtered out parasites which did not share reciprocal breakpoints consistent with shared
289 meiosis.

290
291 Across the dataset we were able to capture one complete tetrad, from infection MAL15 (Figure
292 6). In the absence of complete tetrads it is difficult to definitively conclude parasites came from
293 the same meiosis, or simply share identical parents. However, we found 10 groups of parasites
294 sharing reciprocal breakpoints between 2-4 genotypes (inclusive of the tetrad from MAL15)
295 suggesting they arose from the same meiosis (Data S3). Based on these potential mating's we
296 suggest the minimum number of ookinetes required in an infected mosquito for each infection
297 as between 1 and 5 (Table S1). Importantly, despite exhaustive capture of genetic diversity in
298 nearly all infections, most members of a tetrad do not reach observable frequencies in the blood
299 stream. This suggests there is a considerable attrition in the representation of progeny between
300 the mosquito midgut and the human blood stage. We estimated crossover locations across the
301 dataset using a total of 570 unique crossovers. As seen in previous studies on *P. falciparum*
302 genetic crosses (Jiang et al., 2011) chromosome length and crossover count were correlated
303 ($r^2=0.9$, $p=8.43 \times 10^{-6}$, Pearson's correlation, Figure S7).

304

305 The capture of a complete tetrad allows us to observe non-Mendelian inheritance in a natural
306 malaria genetic cross for the first time. We identified 33 recombination events across the
307 genome, with no cross-overs detected on chromosomes 1,7 and 9. We found evidence for 2
308 major tracts of skewed inheritance resulting from gene conversion. Adjacent to the right-most
309 telomere of chromosome 2 a tract of 872 bp covering 18 markers, and adjacent to the left-most
310 telomere of chromosome 4 a tract of 180,970bp. Within the chromosome 4 region there is a
311 block of 19,432bp from one parent, and 161,538bp from the other. In addition to regions of
312 skewed inheritance we saw 2 large regions (770,168bp on chromosome 8 and 51,426bp on
313 chromosome 9) where variation between the parents had been eliminated by inbreeding. Other
314 regions with no variation distinguishing parents surrounded known hypervariable genes (Miles
315 et al., 2016), and were not included in our analysis.

316 **DISCUSSION**

317
318 There has been a concerted effort to understand the complexity of malaria infections from either
319 deep sequencing data (Assefa et al., 2014, O'Brien et al., 2016, Zhu et al., 2018), or from
320 genotyping a limited number of markers (Chang et al., 2017, Galinsky et al., 2015). We show
321 here there is considerable depth to complex infections which may be challenging to infer from
322 bulk analysis alone. Through a combination of deep sequencing of bulk infections and single-
323 cell sequencing, we have generated the most comprehensive picture of the within-host diversity
324 of malaria infections to date. This provides a much-needed standard for developing novel tools
325 for probing the complexity of infections from deep sequencing data. By using multiple estimates
326 of relatedness targeting distinct features of the data, we argue that most complex infections
327 result from parasites co-transmitted from single mosquito bites in our dataset. Strikingly, our
328 analysis supports only a single infection where simple superinfection of two unrelated strains
329 has occurred (MAL5), and a further three infections where both superinfection and co-
330 transmission have concurrently contributed to diversity (MAL17, MAL24, MAL48). The
331 remaining infections were either monomorphic or showed strong support for co-transmission of
332 related strains only. Notably, the most diverse infection we studied (MAL15) was explained
333 entirely by co-transmission of related parasites. In the two infections where we were unable to
334 capture the minor strains (MAL33 and MAL37), patterns of unfixed SNPs within the infection
335 suggest the uncaptured strain was related to the captured strain (Data S1). It may be that the
336 minor isolate failed to develop to DNA-rich late stages or was present at a fraction lower than
337 we were able to sample within the constraints of this work.

338
339 In this work we have generated a detailed picture of within-host genetic variation across fifteen
340 malaria patients. While this is a modest number of infections, these findings are directly
341 informative about the limits of malaria complexity. We have surveyed a high transmission setting
342 and focused on polyclonal infections. This sampling enriches for infections with the highest
343 likelihood of genetic diversity arising from superinfection rather than co-transmission. In spite of
344 this we find co-transmission to be widespread, and likely underappreciated as a mechanism
345 generating and maintaining genetic diversity in natural malaria populations. There is a pressing
346 need to extend these observations across the range of malaria endemicity to fully capture the
347 transmission network of malaria infections.

348
349 These results could not have been obtained by statistical inference of bulk sequence data
350 alone. There have been impressive advances in imputation of individual parasite haplotypes
351 from bulk sequence data with the development of DEploid (Zhu et al., 2018). We identify two to
352 seventeen haplotypes in the infections we dissect here, with 50% of our infections bearing six or
353 more unique haplotypes. As DEploid typically limits inference to five haplotypes, reliance on
354 bulk inference would have discounted information on the additional haplotypes. When we
355 examine the haplotypes inferred by DEploid we see the accuracy of imputation is not equivalent

356 across all haplotypes in an infection (Figure 3C). Majority haplotypes inferred by DEploid share
357 high similarity (median of 97.8%) to single-cell haplotypes, suggesting DEploid is a highly
358 effective at capturing common haplotypes. However, minority haplotypes (5-50% abundance)
359 were captured poorly (median 84.3% similarity). Encouragingly, we see particularly good
360 performance for DEploid in inferring the composition of a single infection with two unrelated
361 haplotypes (MAL5). The relatively poor performance of inference in other infections suggests
362 that incorporating inbreeding and complex relatedness structures may lead to algorithmic
363 improvements. In general, the data we present here provides an ideal training set for
364 improvements in the implementation of statistical tools for understanding polyclonal infections
365 and in generating guidelines for the interpretation of haplotypes inferred from bulk sequence
366 data.

367
368 Only parasites which transmit gametes to the same mosquito can produce recombinant
369 offspring. Patterns of parasite diversity and relatedness within individual mosquitoes (Annan et
370 al., 2007) (albeit in a distinct population) are in general agreement with our results – most
371 mating is between related parasites. The mechanisms underlying why inbreeding is common,
372 even in high transmission settings, is less clear. Malaria transmission is intense in Chikhwawa
373 (Mzilahowa et al., 2012) and we expected superinfection to be more prevalent than we
374 observed. A mechanism controlling the outcome of superinfection, perhaps by hepcidin based
375 inhibition of liver development in superinfecting sporozoites (Portugal et al., 2011), could explain
376 why we do not see more superinfection. Alternatively, the low numbers of superinfecting
377 parasites emerging from the liver relative to those present in established infections (which may
378 contain 10^{11-12} blood stage parasites) may limit establishment of superinfections. This would
379 represent an infectious disease example of the “priority” effects (De Meester et al., 2016) that
380 are important in determining assemblies of ecological communities or microbiomes. Immune-
381 mediated selection of parasite variants sharing alleles at the major antigenic loci (Farnert et al.,
382 2008) could also generate a strong relatedness structure within infections. However, in this
383 study, the effects of host immunity are likely to be limited because only infections from children
384 who have little or no pre-existing malaria immunity were studied. In analyzing why
385 superinfection is less common, it is also worth noting that analysis of parasite diversity is
386 generally limited to single blood draws due to the need to treat symptomatic patients
387 expediently. As this sampling strategy may overlook sub-populations circulating at lower
388 frequencies, there may be additional genetic variation which escapes routine analysis. Most
389 importantly, the strong relatedness structure we observe will limit the amount of outbreeding in
390 malaria parasites, even in regions of intense transmission. Restrained outbreeding amongst
391 malaria parasites could profoundly shape the evolution of parasite virulence, drug resistance
392 and malaria transmission dynamics as shown in mice (Wargo et al., 2007a, Wargo et al., 2007b,
393 Huijben et al., 2010, Huijben et al., 2011, Alizon, 2013).

394
395 The depletion of genetic variation during repeated rounds of co-transmission has been
396 previously modelled (Wong et al., 2018), suggesting a substantial decline in the number of
397 clonal lineages and an increase in average relatedness can arise through a single transmission
398 cycle. We directly observe this by reconstructing tetrads. In all but one case we do not observe
399 complete tetrads in our data. Some members of the tetrads were either lost during the infection
400 or were present at too low a frequency to be sampled in this study. Either of these scenarios
401 suggest that genetic variation will be depleted over successive transmission cycles, a prospect
402 directly explored in Figure 5. Our data suggest complex infections comprise parasites which
403 have been co-transmitted longer than two transmission cycles. Due to the lengthy
404 developmental cycle of the parasite, and the propensity for mosquitoes to disperse the potential
405 for these patterns to be driven by local population structure is minimal (Conway and McBride,
406 1991, Prugnolle et al., 2008). We observe that substantial genetic variation is maintained

407 despite the bottleneck of mosquito transmission with up to 17 unique haplotypes likely
408 inoculated by a single mosquito. Understanding how patterns of transmission and within host
409 dynamics contribute to the diversity and relatedness structure within malaria infections will help
410 inform ongoing elimination and control efforts.

411 **ACKNOWLEDGEMENTS**

412 We thank all children and their families who participated in this study in Chikhwawa, Malawi. We
413 also thank Andrew Mtande, Ruth Daiman and Miriam Phiri for their help with participant
414 recruitment and clinical management. We are also grateful to Clement Masesa and Lumbani
415 Makhaza for designing our data collection tool and for managing the study database. This study
416 was supported by a Wellcome Trust Intermediate Fellowship in Tropical Medicine and Public
417 Health (Grant # 099992/Z/12/Z to SCN) and an NIH grant (NIAID AI110941-01A1 to IHC). FACS
418 data were generated in the Flow Cytometry Shared Resource Facility (supported by UTHSCSA,
419 NIH-NCI P30 CA054174, UL1RR025767 (CTSA)).
420

421 **AUTHOR CONTRIBUTIONS**

422 S.C.N., S.G.T., S.A.W., D.J.T., T.J.C.A and I.H.C designed the study. S.G.T. and I.H.C.
423 developed tools. S.C.N., S.G.T., K.G., S.N., A.D., C.J., R.G., B.D., and I.H.C. performed
424 experiments. S.C.N., S.K., and D.J.T. collected samples. S.C.N, S.G.T., T.J.C.A and I.H.C.
425 wrote the paper.
426

427 **DECLARATION OF INTERESTS**

428 The authors declare no competing interests. Correspondence and requests for materials should
429 be addressed to ianc@txbiomed.org.
430

431 **Figure Legends**

432 **Figure 1. The within host genetic diversity of malaria parasites is shaped by mosquito**
433 **transmission.** (A) A simple mono-infection is generated when an uninfected individual is bitten
434 by a mosquito bearing a single parasite genotype. (B) A superinfection occurs when an
435 individual is bitten by two mosquitoes, each bearing a single parasite genotype. (C) Co-
436 transmission of parasites occurs when a single mosquito bearing multiple genetically distinct
437 parasites bites an uninfected individual. As genetic recombination is an obligate stage of
438 mosquito transmission multiple related parasites may infect an individual through this route.
439

440 **Figure 2. Complexity of infection inferred from bulk and single-cell sequencing.** (A) F_{WS}
441 scores for 49 bulk sequenced infections. Infections above the dashed line ($F_{WS}=0.95$) are
442 assumed to be clonal. (B) Inferred number of haplotypes (K) inferred by DEploid, infections are
443 ordered by the F_{WS} score. Black dots in (A) and (B) denote infections also deconvoluted by
444 single-cell sequencing. (C) Number of unique haplotypes inferred by single-cell sequencing.
445 This data is included in Table S1.
446

447 **Figure 3. Inferring the composition of malaria infections from bulk sequencing data.**

448 Correlation between the effective number of haplotypes inferred from single-cell sequencing and
449 either F_{WS} (A) or Effective K inferred from DEploid (B). (C) The maximum similarity between
450 each haplotype inferred by DEploid and single-cell sequences from the same infection. The
451 abundance of the haplotype (as estimated by DEploid) for each haplotype is shown on the y-
452 axis. Majority haplotypes were inferred with high accuracy (73.6-99.9% similarity), with reduced
453 accuracy for minority haplotypes. After exclusion of low abundance (<10%) haplotypes and
454 haplotypes from clonal infections there was a significant relationship between abundance and
455 maximum similarity (adjusted $r^2=0.32$, $p=4.6 \times 10^{-5}$, linear model). Clonal infections (MAL29,

456 MAL31, MAL38) and simple superinfections (MAL5) perform uniformly well with DEploid, though
457 other infections show variable success.

458
459 **Figure 4. A network representation of pairwise IBD sharing across the genomes.** Each
460 node represents a single parasite colored by the infection of origin. Nodes are joined if >15% of
461 the genomes are shared IBD. Each node is colored by the infection it was derived from, with
462 bulk sequences denoted by a square and single-cell sequences by a circle. The parasite from a
463 single infection are highlighted by dashed lines. MAL23 and MAL48 both contain multiple
464 unlinked clusters indicative of superinfected parasites.

465
466 **Figure 5. Recent ancestry inferred from IBD sharing.** (A) Density plot of the total IBD shared
467 between parasites from a single infection (labeled to the left of the plot). (B) Density plot of the
468 mean IBD block length between parasites from a single infection. The dotted lines in A and B
469 show the expected value for parasites separated by differing number of meiosis, e.g. clonally
470 identical (~21Mb total IBD/~1.5Mb Mean IBD length) and separated by a single meiosis (~10Mb
471 total IBD/~0.6Mb Mean IBD length). The most distant relationship shown is 5 meiosis. (C)
472 Relative frequency of different degrees of relatedness inferred between parasites from the same
473 infection using the ERSA algorithm (ns - no significant relatedness observed). (D) The number
474 of mitochondrial haplotypes identified in this infection.

475
476 **Figure 6. Patterns of recombination in a tetrad formed during meiosis.** Two parental
477 haplotypes (red and blue) were inferred using Hapi and the inheritance of these haplotypes was
478 inferred in the four parasite genotypes shown here. Across the genome there is consistent 1:1
479 inheritance of parental genomes aside from the proximal end of chromosome 4 and the distal
480 end of chromosome 2 (green boxes, also shown expanded). Inbreeding among the ancestors of
481 the parental genotypes has eroded variation on chromosomes 8 and 9 (orange boxes).

482 STAR METHODS

483 LEAD CONTACT AND MATERIALS AVAILABILITY

484 Further information and requests for resources and reagents should be directed to and will be
485 fulfilled by the Lead Contact, Ian Cheeseman (ianc@txbiomed.org). Raw sequence data has
486 been deposited at the sequence read archive (<https://www.ncbi.nlm.nih.gov/sra>) under study
487 number SRP155167.

488

489 EXPERIMENTAL MODEL AND SUBJECT DETAILS

490 Malaria-infected blood samples (5 ml; thin smear parasitaemia: 0.2 to 21.8%) were obtained
491 prior to treatment from children aged 19 to 116 months old presenting to Chikhwawa District
492 Hospital in Malawi with uncomplicated *P. falciparum* malaria from February to June 2016. Blood
493 samples were collected only from children whose parents or legal guardians provided consent.
494 Ethical approval for this study was obtained from the University of Malawi College of Medicine
495 Research and Ethics Committee (Protocol number P.02/13/1528) and the Liverpool School of
496 Tropical Medicine Research Ethics Committee (Protocol number 14.035). Each research
497 subject was assigned a unique ID number at the time of enrollment. Similarly, each blood
498 sample was assigned a unique barcode at the time of collection. The sample barcode was used
499 to identify and track each sample while being processed and analyzed in the laboratory.
500 Detailed information about all research subjects and blood samples they donated are provided
501 in Table S1.

502

503 METHOD DETAILS

504

505 Sample Collection

506 Venous blood (5ml) from each subject was collected directly into an Acid Citrate Dextrose tube
507 (BD, UK). The sample was immediately placed in an ice-cold container and transported to our
508 laboratory in Blantyre within six hours of collection. Half of each blood sample was washed
509 using incomplete RPMI 1640 media (Sigma-Aldrich, UK). Three aliquots of the sample were
510 cryopreserved in glycerolyte 57 solution (Fenwal, Lake Zurich, IL, USA) and stored in liquid
511 nitrogen. Parasites used in fluorescence-activated single-cell sorting were cultured from one of
512 these aliquots. The second half of the sample was filtered using CF11 columns to deplete
513 human leucocytes (Venkatesan et al., 2012), and was stored at -80°C until needed. Parasite
514 DNA was extracted from this sample using a DNA Mini Kit (QIAGEN, USA) and directly
515 sequenced on an Illumina HiSeq instrument.

516

517 **Single-cell capture**

518 We performed single-cell capture, whole genome amplification, sequencing analysis and
519 followed guidelines for preventing contamination using the approaches described in (Nair et al.,
520 2014, Trevino et al., 2017). We outline these approaches below.

521

522 *Parasite culture*

523 Approximately 1 mL of cryopreserved blood sample was thawed at 37°C to revive intact cells
524 (~200ul recovered pellet, ~1% parasitemia). The sample was washed twice by adding 10mL of
525 complete media (filter-sterilized incomplete RPMI 1640 media to which 5% w/v of hypoxanthine
526 and 8% w/v of albumax II were added). Following the final centrifugation step (425 x g for 5
527 minutes) cells were resuspended and grown in 8 mL complete media in a sealed T25 tissue
528 culture flask flushed with 5% CO₂, 5% O₂ and 90% N₂ prior to being sealed. The culture flask
529 was incubated at 37°C for 40 hours to allow for parasite progression to late stages, which
530 generates higher quality genomic data after MDA and library preparation (Trevino et al., 2017).
531 To stain parasitized cells in readiness for FACS, ~8 µl of an infected red blood cell pellet (~10⁸
532 cells) was resuspended in 10 mL of 1X PBS (Lonza, USA) which included 5 µl of Vibrant
533 DyeCycle Green at 37°C for 30 minutes with intermittent manual inversion of the tube
534 approximately every 10 minutes. Cells were washed once in 1X PBS and resuspended in 5 - 8
535 mL of 1X PBS in a foil-covered tube to protect the dye from photobleaching in preparation for
536 FACS sorting. Catalog numbers for the critical reagents used in parasite culture and capture of
537 single parasitized cells are provided in the *Key Resources Table*.

538

539 *FACS Sorting*

540 Cells were sorted by MoFlo Astrios (Beckman Coulter) by gating the two brightest observed
541 populations according to DNA fluorescence, the sort was run in single-cell sort mode with a drop
542 envelope of 0.5. Individual cells were sorted into 0.2 mL PCR tubes containing 5 µl autoclaved
543 sterile PBS (Lonza), which had been prepared under sterile conditions in a PCR hood. Each
544 event required about 15 seconds to open the tube, place on the sorting rack, recover, and close
545 the tube. Tubes were then immediately stored on dry ice and transferred to -80 °C longer-term
546 storage within an hour.

547

548 **Generation of single-cell DNA libraries**

549 Library preparation for individually sorted late-stage parasites was carried out using the Qiagen
550 Single-Cell FX DNA kit without library amplification according to manufacturer's instructions.
551 Whole genome amplification preparation was carried out under a PCR hood and DNA was
552 amplified on a dedicated PCR machine. Library products were analyzed by TapeStation and
553 included off-target peaks typical of MDA DNA inputs. Adapter-ligated DNA products were
554 quantified by KAPA Hyperplus Kits. All sequencing was performed on an Illumina HiSeq 2500. A
555 detailed description of the development of the single-cell sequencing methods used here, and
556 the protocols in place to control for contamination are available (Nair et al., 2014, Trevino et al.,

557 2017). Raw sequence data has been deposited at the sequence read archive
558 (<https://www.ncbi.nlm.nih.gov/sra>) under study number SRP155167.

559
560

Sequence analysis

561 We aligned raw sequencing reads to v3 of the 3D7 genome reference
562 (<http://www.plasmodb.org>) using BWA MEM v0.7.5a (Li, 2013). After removing PCR duplicates
563 and reads mapping to the ends of chromosomes (Picard v1.56) we recalibrated base quality
564 scores, realigned around indels and called genotypes using GATK v3.5 (DePristo et al., 2011) in
565 the GenotypeGVCFs mode using QualByDepth, FisherStrand, StrandOddsRatio VariantType,
566 GC Content and max_alterate_alleles set to 6. We recalibrated quality scores and calculated
567 VQSLOD scores using SNP calls conforming to Mendelian inheritance, excluding sites where
568 the VQSLOD score was <0. Median read depth of WGA single-cells was 28.3 (interquartile
569 range (IQR) 12.5-46.4) with median of 90.5% (IQR 78.1-96.0%) of the genome covered by at
570 least one read. In contrast the non-WGA samples had a median read depth of 31.11 (IQR
571 20.93-48.37) and a median of 95.8% (IQR 93.1-97.4%) of the genome covered by at least one
572 read. A potential source of error in single-cell genomics is the inclusion of exogenous DNA
573 amplified alongside the target genome in downstream analysis. As an initial indication of the
574 potential of non-target DNA being introduced to our analysis we first examined the proportion of
575 reads mapping to the *P. falciparum* genome (Gardner et al., 2002) in each sequence. We
576 observed a median of 93.3% (IQR 87.0-95.4%) of reads map to the parasite genome for single-
577 cell sequences, compared to 35.7% (IQR 19.7-48.5%) for bulk patient samples and 79.4% (IQR
578 74.5-86.9%) for clonally expanded samples suggesting our stringent handling protocols were
579 effective at eliminating environmental DNA. For a more rigorous test we identified lines with
580 potential cross contamination based on unfixed basecall frequency. As the parasite genome is
581 haploid during blood stages all variants are expected to be fixed in genome sequencing data.
582 The highly AT-rich and repetitive nature of the parasite genome makes alignment challenging,
583 generating false positive unfixed variants in clonal lines. After excluding highly error-prone
584 genomic regions (calls outside of the “core genome”(Miles et al., 2016) or within microsatellites)
585 we measured the proportion of mixed base calls (>5% of reads at a locus mapping to the
586 minority allele) at high confidence biallelic SNPs (>10 reads mapped, VQSLOD>0, GQ>70).
587 Using the cloned lines and bulk population samples as a guide we estimated 1% as an
588 appropriate threshold for excluding putatively mixed lines (Figure S1).

589
590

QUANTIFICATION AND STATISTICAL ANALYSIS

Estimating the complexity and diversity of bulk sequenced samples

591 F_{WS} was calculated in moimix (<https://github.com/bahlolab/moimix>) for all bulk patient samples.
592 We estimated the number of unique haplotypes and their sequence from deep sequence of bulk
593 infections using DEploid (Zhu et al., 2018) v0.5 (<https://github.com/mcveanlab/DEploid>). We
594 used 10,997 HQ SNPs with a MAF >5%. For a reference panel we used 10 bulk Malawian
595 samples presumed to be clonal ($F_{WS}>0.95$) and population level allele frequencies from across
596 the complete bulk sequencing data. We inferred the most likely number of haplotypes (K) using
597 the command:

598

```
599 ./dEplod -ref sample_reference_allele_counts.txt -alt sample_alternative_allele_counts.txt -plaf  
600 population_allele_freq.txt -o sample_out -ibd -noPanel -exclude highly_variable_sites.txt -sigma  
601 7 -seed 2
```

602
603
604

Estimating relatedness between sequences

605 SNP data were imported into R using SeqArray (Zheng et al., 2017). Between all samples
606 passing quality control we calculated the proportion of shared alleles and using SNPs which

607 were at >5% MAF in the bulk sequenced samples. We used a distance matrix generated from
608 this data (1-pairwise allele sharing) to estimate the number of unique haplotypes in each
609 infection by collapsing together sequences which differed at <1% of sites. Rarefaction of
610 haplotype abundance was performed using the rareNMtests package (Cayuela and Gotelli,
611 2014) in R. We called regions of IBD between all samples passing quality control using hmmlBD
612 v2.0.0 (Schaffner et al., 2018) (<https://github.com/glipsnort/hmmlBD>). We performed maximum-
613 likelihood estimation of recent shared ancestry using ERSA 2.0 (Huff et al., 2011, Li et al., 2014)
614 (<http://www.hufflab.org/software/ersa/>) using the output from hmmlBD using the flags --
615 min_cm=1.5 --adjust_pop_dist=true --number_of_chromosomes=14 --rec_per_meioses=19. We
616 converted the basepair positions to a uniform genetic map using the scaling factor 1cM=9.6kb
617 (Jiang et al., 2011) and excluded IBD chunks <1cM in length. As identical clones are not
618 specifically modelled in ERSA we excluded these from analysis, though their abundance is
619 shown in the '0' bar in Figure 5C. All other statistical analysis and visualization was performed in
620 R v3.4.0 (Team, 2017). Inference of parental genotypes and recombination breakpoints was
621 performed using Hapi.

622

623 DATA AND CODE AVAILABILITY

624 This study did not generate any novel code. The data generated during this study are available
625 from the sequence read archive (<https://www.ncbi.nlm.nih.gov/sra>) under study number
626 SRP155167.

627

628 REFERENCES

- 629 ALIZON, S. 2013. Parasite co-transmission and the evolutionary epidemiology of virulence.
630 *Evolution*, 67, 921-33.
- 631 ANNAN, Z., DURAND, P., AYALA, F. J., ARNATHAU, C., AWONO-AMBENE, P., SIMARD, F.,
632 RAZAKANDRAINIBE, F. G., KOELLA, J. C., FONTENILLE, D. & RENAUD, F. 2007.
633 Population genetic structure of Plasmodium falciparum in the two main African vectors,
634 Anopheles gambiae and Anopheles funestus. *Proc Natl Acad Sci U S A*, 104, 7987-92.
- 635 ASSEFA, S. A., PRESTON, M. D., CAMPINO, S., OCHOLLA, H., SUTHERLAND, C. J. &
636 CLARK, T. G. 2014. estMOI: estimating multiplicity of infection using parasite deep
637 sequencing data. *Bioinformatics*, 30, 1292-4.
- 638 AUBURN, S., CAMPINO, S., MIOTTO, O., DJIMDE, A. A., ZONGO, I., MANSKE, M., MASLEN,
639 G., MANGANO, V., ALCOCK, D., MACINNIS, B., ROCKETT, K. A., CLARK, T. G.,
640 DOUMBO, O. K., OUEDRAOGO, J. B. & KWIATKOWSKI, D. P. 2012. Characterization
641 of within-host Plasmodium falciparum diversity using next-generation sequence data.
642 *PLoS One*, 7, e32891.
- 643 BELL, A. S., DE ROODE, J. C., SIM, D. & READ, A. F. 2006. Within-host competition in
644 genetically diverse malaria infections: parasite virulence and competitive success.
645 *Evolution*, 60, 1358-71.
- 646 BRIGHT, A. T., MANARY, M. J., TEWHEY, R., ARANGO, E. M., WANG, T., SCHORK, N. J.,
647 YANOW, S. K. & WINZELER, E. A. 2014. A high resolution case study of a patient with
648 recurrent Plasmodium vivax infections shows that relapses were caused by meiotic
649 siblings. *PLoS Negl Trop Dis*, 8, e2882.
- 650 CAYUELA, L. & GOTELLI, N. J. 2014. rareNMtests: Ecological and biogeographical null model
651 tests for comparing rarefaction curves.
- 652 CHANG, H. H., WORBY, C. J., YEKA, A., NANKABIRWA, J., KAMYA, M. R., STAEDKE, S. G.,
653 DORSEY, G., MURPHY, M., NEAFSEY, D. E., JEFFREYS, A. E., HUBBART, C.,
654 ROCKETT, K. A., AMATO, R., KWIATKOWSKI, D. P., BUCKEE, C. O. &
655 GREENHOUSE, B. 2017. THE REAL McCOIL: A method for the concurrent estimation

656 of the complexity of infection and SNP allele frequency for malaria parasites. *PLoS*
657 *Comput Biol*, 13, e1005348.

658 COLE, F., BAUDAT, F., GREY, C., KEENEY, S., DE MASSY, B. & JASIN, M. 2014. Mouse
659 tetrad analysis provides insights into recombination mechanisms and hotspot
660 evolutionary dynamics. *Nat Genet*, 46, 1072-80.

661 CONWAY, D. J., GREENWOOD, B. M. & MCBRIDE, J. S. 1991. The epidemiology of multiple-
662 clone Plasmodium falciparum infections in Gambian patients. *Parasitology*, 103 Pt 1, 1-
663 6.

664 CONWAY, D. J. & MCBRIDE, J. S. 1991. Genetic evidence for the importance of interrupted
665 feeding by mosquitoes in the transmission of malaria. *Trans R Soc Trop Med Hyg*, 85,
666 454-6.

667 DE MEESTER, L., VANOVERBEKE, J., KILSDONK, L. J. & URBAN, M. C. 2016. Evolving
668 Perspectives on Monopolization and Priority Effects. *Trends Ecol Evol*, 31, 136-146.

669 DE ROODE, J. C., PANSINI, R., CHEESMAN, S. J., HELINSKI, M. E., HUIJBEN, S., WARGO,
670 A. R., BELL, A. S., CHAN, B. H., WALLIKER, D. & READ, A. F. 2005. Virulence and
671 competitive ability in genetically diverse malaria infections. *Proc Natl Acad Sci U S A*,
672 102, 7624-8.

673 DEPRISTO, M. A., BANKS, E., POPLIN, R., GARIMELLA, K. V., MAGUIRE, J. R., HARTL, C.,
674 PHILIPPAKIS, A. A., DEL ANGEL, G., RIVAS, M. A., HANNA, M., MCKENNA, A.,
675 FENNEL, T. J., KERNYTSKY, A. M., SIVACHENKO, A. Y., CIBULSKIS, K., GABRIEL,
676 S. B., ALTSHULER, D. & DALY, M. J. 2011. A framework for variation discovery and
677 genotyping using next-generation DNA sequencing data. *Nat Genet*, 43, 491-8.

678 DHARIA, N. V., PLOUFFE, D., BOPP, S. E., GONZALEZ-PAEZ, G. E., LUCAS, C., SALAS, C.,
679 SOBERON, V., BURSULAYA, B., KOCHER, T. J., BACON, D. J. & WINZELER, E. A.
680 2010. Genome scanning of Amazonian Plasmodium falciparum shows subtelomeric
681 instability and clindamycin-resistant parasites. *Genome Res*, 20, 1534-44.

682 EARLY, A. M., LIEVENS, M., MACINNIS, B. L., OCKENHOUSE, C. F., VOLKMAN, S. K.,
683 ADJEI, S., AGBENYEGA, T., ANSONG, D., GONDI, S., GREENWOOD, B., HAMEL, M.,
684 ODERO, C., OTIENO, K., OTIENO, W., OWUSU-AGYEI, S., ASANTE, K. P., SORGHO,
685 H., TINA, L., TINTO, H., VALEA, I., WIRTH, D. F. & NEAFSEY, D. E. 2018. Host-
686 mediated selection impacts the diversity of Plasmodium falciparum antigens within
687 infections. *Nat Commun*, 9, 1381.

688 FARNERT, A., LEBBAD, M., FARAJA, L. & ROTH, I. 2008. Extensive dynamics of
689 Plasmodium falciparum densities, stages and genotyping profiles. *Malar J*, 7, 241.

690 GALINSKY, K., VALIM, C., SALMIER, A., DE THOISY, B., MUSSET, L., LEGRAND, E.,
691 FAUST, A., BANIECKI, M. L., NDIAYE, D., DANIELS, R. F., HARTL, D. L., SABETI, P.
692 C., WIRTH, D. F., VOLKMAN, S. K. & NEAFSEY, D. E. 2015. COIL: a methodology for
693 evaluating malarial complexity of infection using likelihood from single nucleotide
694 polymorphism data. *Malar J*, 14, 4.

695 GARDNER, M. J., HALL, N., FUNG, E., WHITE, O., BERRIMAN, M., HYMAN, R. W.,
696 CARLTON, J. M., PAIN, A., NELSON, K. E., BOWMAN, S., PAULSEN, I. T., JAMES, K.,
697 EISEN, J. A., RUTHERFORD, K., SALZBERG, S. L., CRAIG, A., KYES, S., CHAN, M.
698 S., NENE, V., SHALLOM, S. J., SUH, B., PETERSON, J., ANGIUOLI, S., PERTEA, M.,
699 ALLEN, J., SELENGUT, J., HAFT, D., MATHER, M. W., VAIDYA, A. B., MARTIN, D. M.,
700 FAIRLAMB, A. H., FRAUNHOLZ, M. J., ROOS, D. S., RALPH, S. A., MCFADDEN, G. I.,
701 CUMMINGS, L. M., SUBRAMANIAN, G. M., MUNGALL, C., VENTER, J. C., CARUCCI,
702 D. J., HOFFMAN, S. L., NEWBOLD, C., DAVIS, R. W., FRASER, C. M. & BARRELL, B.
703 2002. Genome sequence of the human malaria parasite Plasmodium falciparum. *Nature*,
704 419, 498-511.

705 HENDEN, L., LEE, S., MUELLER, I., BARRY, A. & BAHLO, M. 2018. Identity-by-descent
706 analyses for measuring population dynamics and selection in recombining pathogens.
707 *PLoS Genet*, 14, e1007279.

708 HOU, Y., FAN, W., YAN, L., LI, R., LIAN, Y., HUANG, J., LI, J., XU, L., TANG, F., XIE, X. S. &
709 QIAO, J. 2013. Genome analyses of single human oocytes. *Cell*, 155, 1492-506.

710 HUFF, C. D., WITHERSPOON, D. J., SIMONSON, T. S., XING, J., WATKINS, W. S., ZHANG,
711 Y., TUOHY, T. M., NEKLASON, D. W., BURT, R. W., GUTHERY, S. L., WOODWARD,
712 S. R. & JORDE, L. B. 2011. Maximum-likelihood estimation of recent shared ancestry
713 (ERSA). *Genome Res*, 21, 768-74.

714 HUIJBEN, S., NELSON, W. A., WARGO, A. R., SIM, D. G., DREW, D. R. & READ, A. F. 2010.
715 Chemotherapy, within-host ecology and the fitness of drug-resistant malaria parasites.
716 *Evolution*, 64, 2952-68.

717 HUIJBEN, S., SIM, D. G., NELSON, W. A. & READ, A. F. 2011. The fitness of drug-resistant
718 malaria parasites in a rodent model: multiplicity of infection. *J Evol Biol*, 24, 2410-22.

719 JIANG, H., LI, N., GOPALAN, V., ZILVERSMIT, M. M., VARMA, S., NAGARAJAN, V., LI, J.,
720 MU, J., HAYTON, K., HENSCHEN, B., YI, M., STEPHENS, R., MCVEAN, G.,
721 AWADALLA, P., WELLEMS, T. E. & SU, X. Z. 2011. High recombination rates and
722 hotspots in a Plasmodium falciparum genetic cross. *Genome Biol*, 12, R33.

723 LEUNG, M. L., WANG, Y., WATERS, J. & NAVIN, N. E. 2015. SNES: single nucleus exome
724 sequencing. *Genome Biol*, 16, 55.

725 LI, H., GLUSMAN, G., HU, H., SHANKARACHARYA, CABALLERO, J., HUBLEY, R.,
726 WITHERSPOON, D., GUTHERY, S. L., MAULDIN, D. E., JORDE, L. B., HOOD, L.,
727 ROACH, J. C. & HUFF, C. D. 2014. Relationship estimation from whole-genome
728 sequence data. *PLoS Genet*, 10, e1004144.

729 LI, H. J. A. P. A. 2013. Aligning sequence reads, clone sequences and assembly contigs with
730 BWA-MEM.

731 LI, R., QU, H., CHEN, J., WANG, S., CHATER, J. M., ZHANG, L., WEI, J., ZHANG, Y.-M., XU,
732 C., ZHONG, W.-D., ZHU, J., LU, J., MA, R., FERRANTE, S. P., ROOSE, M. L. & JIA, Z.
733 2018. Inference of Chromosome-length Haplotypes using Genomic Data of Three to
734 Five Single Gametes. *bioRxiv*.

735 LI, X., LI, L. & YAN, J. 2015. Dissecting meiotic recombination based on tetrad analysis by
736 single-microspore sequencing in maize. *Nat Commun*, 6, 6648.

737 LU, S., ZONG, C., FAN, W., YANG, M., LI, J., CHAPMAN, A. R., ZHU, P., HU, X., XU, L., YAN,
738 L., BAI, F., QIAO, J., TANG, F., LI, R. & XIE, X. S. 2012. Probing meiotic recombination
739 and aneuploidy of single sperm cells by whole-genome sequencing. *Science*, 338, 1627-
740 30.

741 MANCERA, E., BOURGON, R., HUBER, W. & STEINMETZ, L. M. 2011. Genome-wide survey
742 of post-meiotic segregation during yeast recombination. *Genome Biol*, 12, R36.

743 MANSKE, M., MIOTTO, O., CAMPINO, S., AUBURN, S., ALMAGRO-GARCIA, J., MASLEN,
744 G., O'BRIEN, J., DJIMDE, A., DOUMBO, O., ZONGO, I., OUEDRAOGO, J. B.,
745 MICHON, P., MUELLER, I., SIBA, P., NZILA, A., BORRMANN, S., KIARA, S. M.,
746 MARSH, K., JIANG, H., SU, X. Z., AMARATUNGA, C., FAIRHURST, R., SOCHEAT, D.,
747 NOSTEN, F., IMWONG, M., WHITE, N. J., SANDERS, M., ANASTASI, E., ALCOCK, D.,
748 DRURY, E., OYOLA, S., QUAIL, M. A., TURNER, D. J., RUANO-RUBIO, V., JYOTHI,
749 D., AMENGA-ETEGO, L., HUBBART, C., JEFFREYS, A., ROWLANDS, K.,
750 SUTHERLAND, C., ROPER, C., MANGANO, V., MODIANO, D., TAN, J. C., FERDIG,
751 M. T., AMAMBUA-NGWA, A., CONWAY, D. J., TAKALA-HARRISON, S., PLOWE, C. V.,
752 RAYNER, J. C., ROCKETT, K. A., CLARK, T. G., NEWBOLD, C. I., BERRIMAN, M.,
753 MACINNIS, B. & KWIATKOWSKI, D. P. 2012. Analysis of Plasmodium falciparum
754 diversity in natural infections by deep sequencing. *Nature*, 487, 375-9.

755 MILES, A., IQBAL, Z., VAUTERIN, P., PEARSON, R., CAMPINO, S., THERON, M., GOULD,
756 K., MEAD, D., DRURY, E., O'BRIEN, J., RUANO RUBIO, V., MACINNIS, B., MWANGI,
757 J., SAMARAKOON, U., RANFORD-CARTWRIGHT, L., FERDIG, M., HAYTON, K., SU,
758 X. Z., WELLEMS, T., RAYNER, J., MCVEAN, G. & KWIATKOWSKI, D. 2016. Indels,
759 structural variation, and recombination drive genomic diversity in *Plasmodium*
760 *falciparum*. *Genome Res*, 26, 1288-99.

761 MU, J., AWADALLA, P., DUAN, J., MCGEE, K. M., JOY, D. A., MCVEAN, G. A. & SU, X. Z.
762 2005. Recombination hotspots and population structure in *Plasmodium falciparum*. *PLoS*
763 *Biol*, 3, e335.

764 MU, J., AWADALLA, P., DUAN, J., MCGEE, K. M., KEEBLER, J., SEYDEL, K., MCVEAN, G. A.
765 & SU, X. Z. 2007. Genome-wide variation and identification of vaccine targets in the
766 *Plasmodium falciparum* genome. *Nat Genet*, 39, 126-30.

767 MZILAHOWA, T., HASTINGS, I. M., MOLYNEUX, M. E. & MCCALL, P. J. 2012. Entomological
768 indices of malaria transmission in Chikhwawa district, Southern Malawi. *Malar J*, 11,
769 380.

770 NAIR, S., NKHOMA, S. C., SERRE, D., ZIMMERMAN, P. A., GORENA, K., DANIEL, B. J.,
771 NOSTEN, F., ANDERSON, T. J. & CHEESEMAN, I. H. 2014. Single-cell genomics for
772 dissection of complex malaria infections. *Genome Res*, 24, 1028-38.

773 NEAFSEY, D. E., SCHAFFNER, S. F., VOLKMAN, S. K., PARK, D., MONTGOMERY, P.,
774 MILNER, D. A., JR., LUKENS, A., ROSEN, D., DANIELS, R., HOUDE, N., CORTESE, J.
775 F., TYNDALL, E., GATES, C., STANGE-THOMANN, N., SARR, O., NDIAYE, D., NDIR,
776 O., MBOUP, S., FERREIRA, M. U., MORAES SDO, L., DASH, A. P., CHITNIS, C. E.,
777 WIEGAND, R. C., HARTL, D. L., BIRREN, B. W., LANDER, E. S., SABETI, P. C. &
778 WIRTH, D. F. 2008. Genome-wide SNP genotyping highlights the role of natural
779 selection in *Plasmodium falciparum* population divergence. *Genome Biol*, 9, R171.

780 NKHOMA, S. C., NAIR, S., CHEESEMAN, I. H., ROHR-ALLEGRI, C., SINGLAM, S.,
781 NOSTEN, F. & ANDERSON, T. J. 2012. Close kinship within multiple-genotype malaria
782 parasite infections. *Proc Biol Sci*, 279, 2589-98.

783 O'BRIEN, J. D., IQBAL, Z., WENDLER, J. & AMENGA-ETEGO, L. 2016. Inferring Strain Mixture
784 within Clinical *Plasmodium falciparum* Isolates from Genomic Sequence Data. *PLoS*
785 *Comput Biol*, 12, e1004824.

786 PEARSON, R. D., AMATO, R., AUBURN, S., MIOTTO, O., ALMAGRO-GARCIA, J.,
787 AMARATUNGA, C., SUON, S., MAO, S., NOVIYANTI, R., TRIMARSANTO, H.,
788 MARFURT, J., ANSTEY, N. M., WILLIAM, T., BONI, M. F., DOLECEK, C., HIEN, T. T.,
789 WHITE, N. J., MICHON, P., SIBA, P., TAVUL, L., HARRISON, G., BARRY, A.,
790 MUELLER, I., FERREIRA, M. U., KARUNAWEEERA, N., RANDRIANARIVELOJOSIA,
791 M., GAO, Q., HUBBART, C., HART, L., JEFFERY, B., DRURY, E., MEAD, D., KEKRE,
792 M., CAMPINO, S., MANSKE, M., CORNELIUS, V. J., MACINNIS, B., ROCKETT, K. A.,
793 MILES, A., RAYNER, J. C., FAIRHURST, R. M., NOSTEN, F., PRICE, R. N. &
794 KWIATKOWSKI, D. P. 2016. Genomic analysis of local variation and recent evolution in
795 *Plasmodium vivax*. *Nat Genet*, 48, 959-964.

796 PORTUGAL, S., CARRET, C., RECKER, M., ARMITAGE, A. E., GONCALVES, L. A.,
797 EPIPHANIO, S., SULLIVAN, D., ROY, C., NEWBOLD, C. I., DRAKESMITH, H. & MOTA,
798 M. M. 2011. Host-mediated regulation of superinfection in malaria. *Nat Med*, 17, 732-7.

799 PRUGNOLLE, F., DURAND, P., JACOB, K., RAZAKANDRAINIBE, F., ARNATHAU, C.,
800 VILLARREAL, D., ROUSSET, F., DE MEEUS, T. & RENAUD, F. 2008. A comparison of
801 *Anopheles gambiae* and *Plasmodium falciparum* genetic structure over space and time.
802 *Microbes Infect*, 10, 269-75.

803 REECE, S. E., DREW, D. R. & GARDNER, A. 2008. Sex ratio adjustment and kin discrimination
804 in malaria parasites. *Nature*, 453, 609-14.

805 REILLY, H. B., WANG, H., STEUTER, J. A., MARX, A. M. & FERDIG, M. T. 2007. Quantitative
806 dissection of clone-specific growth rates in cultured malaria parasites. *Int J Parasitol*, 37,
807 1599-607.

808 ROSARIO, V. 1981. Cloning of naturally occurring mixed infections of malaria parasites.
809 *Science*, 212, 1037-8.

810 SCHAFFNER, S. F., TAYLOR, A. R., WONG, W., WIRTH, D. F. & NEAFSEY, D. E. 2018.
811 hmmlBD: software to infer pairwise identity by descent between haploid genotypes.
812 *Malar J*, 17, 196.

813 TEAM, R. C. 2017. R: A Language and Environment for Statistical Computing.

814 TREVINO, S. G., NKHOMA, S. C., NAIR, S., DANIEL, B. J., MONCADA, K., KHOSWE, S.,
815 BANDA, R. L., NOSTEN, F. & CHEESEMAN, I. H. 2017. High-Resolution Single-Cell
816 Sequencing of Malaria Parasites. *Genome Biol Evol*, 9, 3373-3383.

817 VOLKMAN, S. K., NEAFSEY, D. E., SCHAFFNER, S. F., PARK, D. J. & WIRTH, D. F. 2012.
818 Harnessing genomics and genome biology to understand malaria biology. *Nat Rev*
819 *Genet*, 13, 315-28.

820 WARGO, A. R., DE ROODE, J. C., HUIJBEN, S., DREW, D. R. & READ, A. F. 2007a.
821 Transmission stage investment of malaria parasites in response to in-host competition.
822 *Proc Biol Sci*, 274, 2629-38.

823 WARGO, A. R., HUIJBEN, S., DE ROODE, J. C., SHEPHERD, J. & READ, A. F. 2007b.
824 Competitive release and facilitation of drug-resistant parasites after therapeutic
825 chemotherapy in a rodent malaria model. *Proc Natl Acad Sci U S A*, 104, 19914-9.

826 WHO 2016. *World malaria report 2015*, World Health Organization.

827 WONG, W., GRIGGS, A. D., DANIELS, R. F., SCHAFFNER, S. F., NDIAYE, D., BEI, A. K.,
828 DEME, A. B., MACINNIS, B., VOLKMAN, S. K., HARTL, D. L., NEAFSEY, D. E. &
829 WIRTH, D. F. 2017. Genetic relatedness analysis reveals the cotransmission of
830 genetically related Plasmodium falciparum parasites in Thies, Senegal. *Genome Med*, 9,
831 5.

832 WONG, W., WENGER, E. A., HARTL, D. L. & WIRTH, D. F. 2018. Modeling the genetic
833 relatedness of Plasmodium falciparum parasites following meiotic recombination and
834 cotransmission. *PLoS Comput Biol*, 14, e1005923.

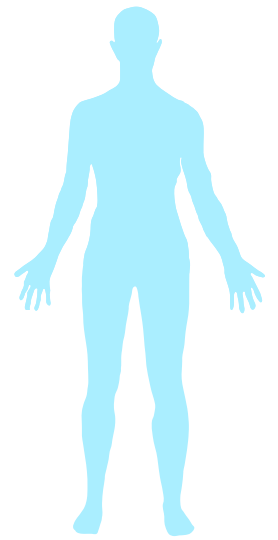
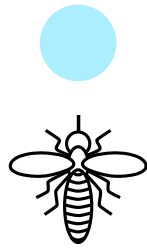
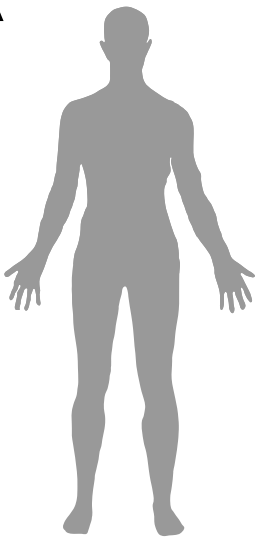
835 ZHENG, X., GOGARTEN, S. M., LAWRENCE, M., STILP, A., CONOMOS, M. P., WEIR, B. S.,
836 LAURIE, C. & LEVINE, D. 2017. SeqArray-a storage-efficient high-performance data
837 format for WGS variant calls. *Bioinformatics*, 33, 2251-2257.

838 ZHU, S. J., ALMAGRO-GARCIA, J. & MCVEAN, G. 2018. Deconvolution of multiple infections
839 in Plasmodium falciparum from high throughput sequencing data. *Bioinformatics*, 34, 9-
840 15.

841

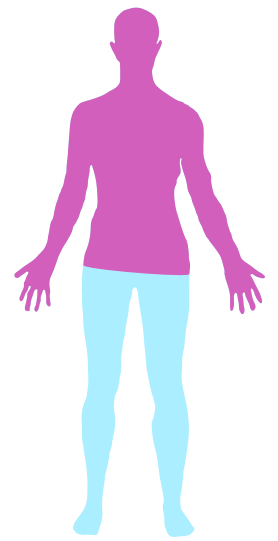
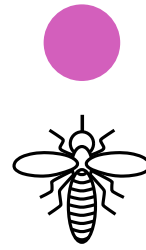
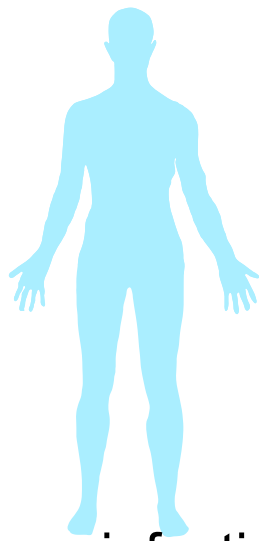
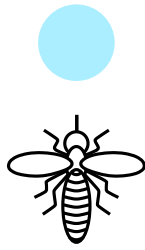
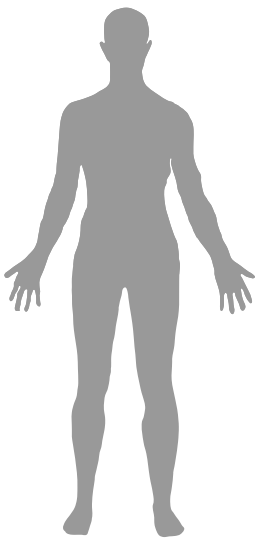
Figure 1

A



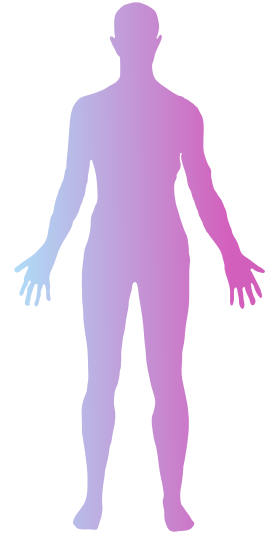
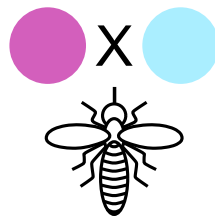
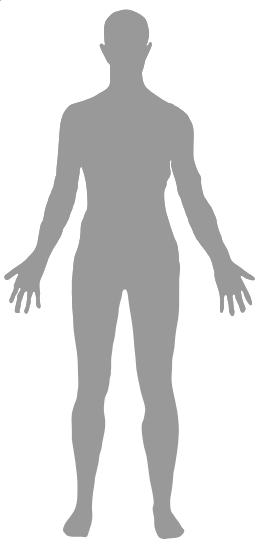
mono-infection

B



superinfection

C



co-transmission

Figure 2

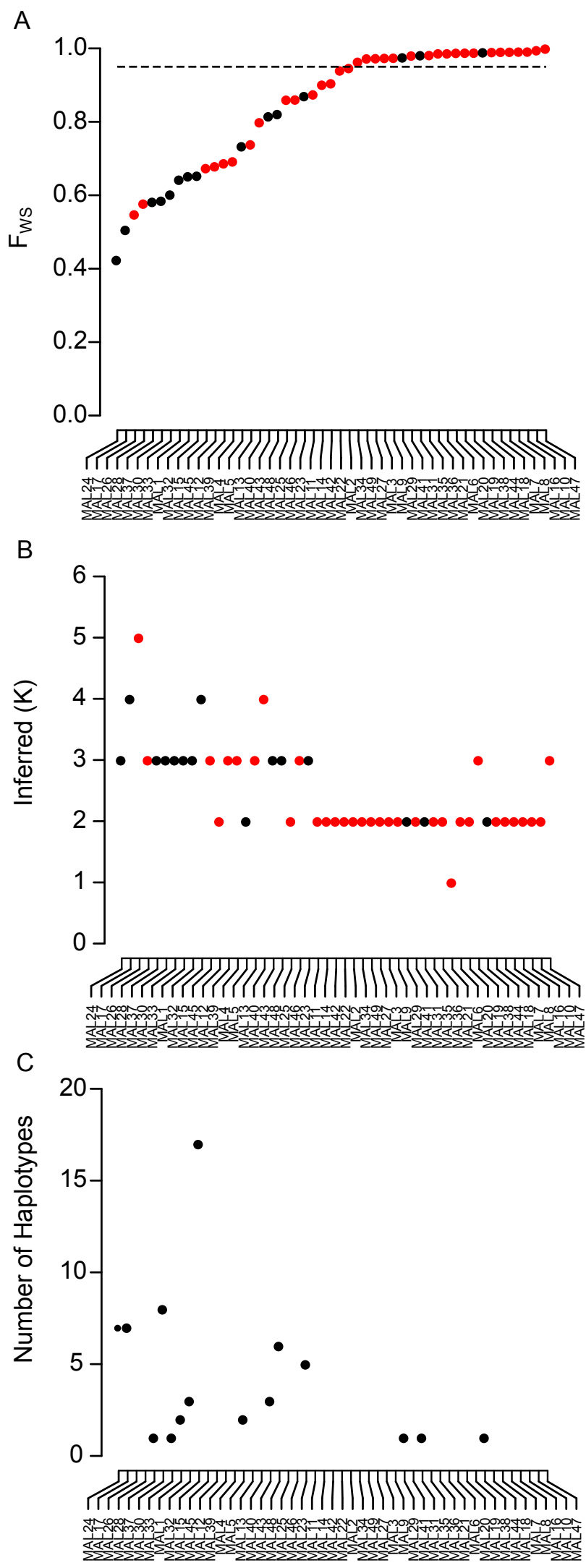


Figure 3

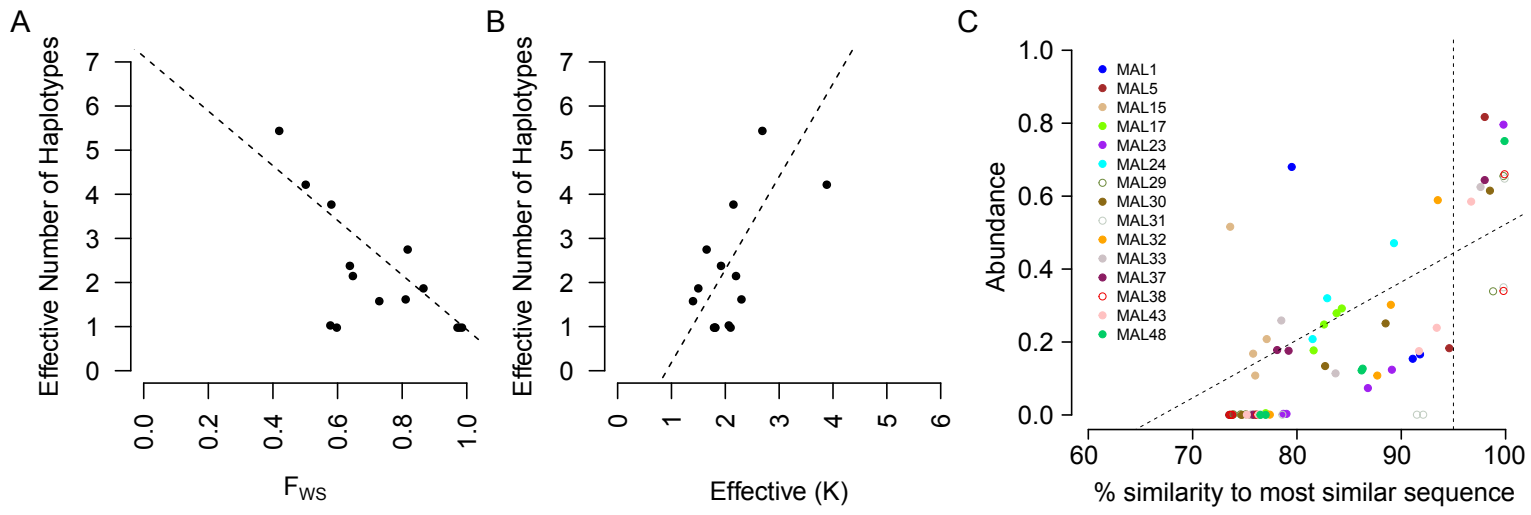


Figure 4

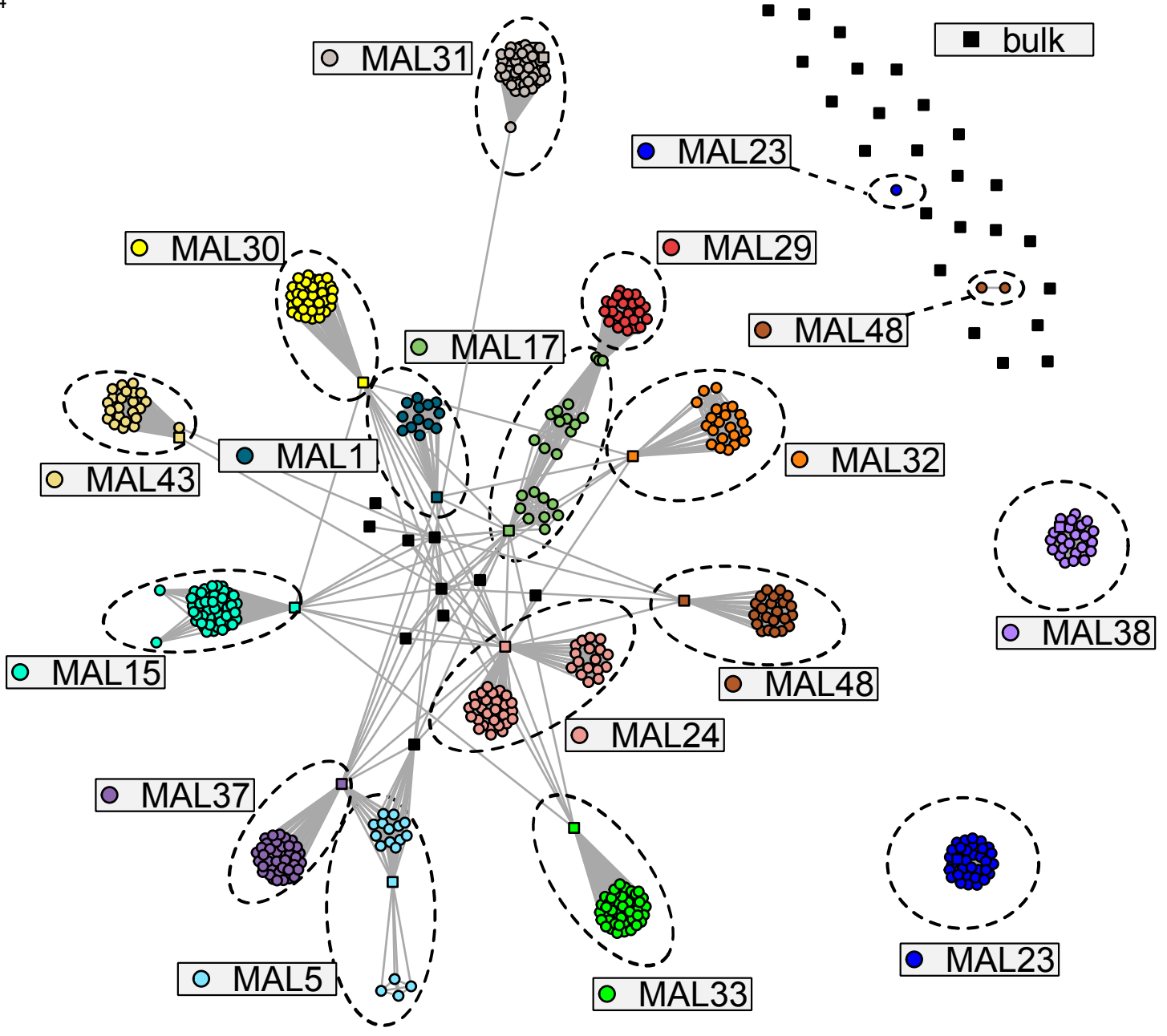


Figure 5

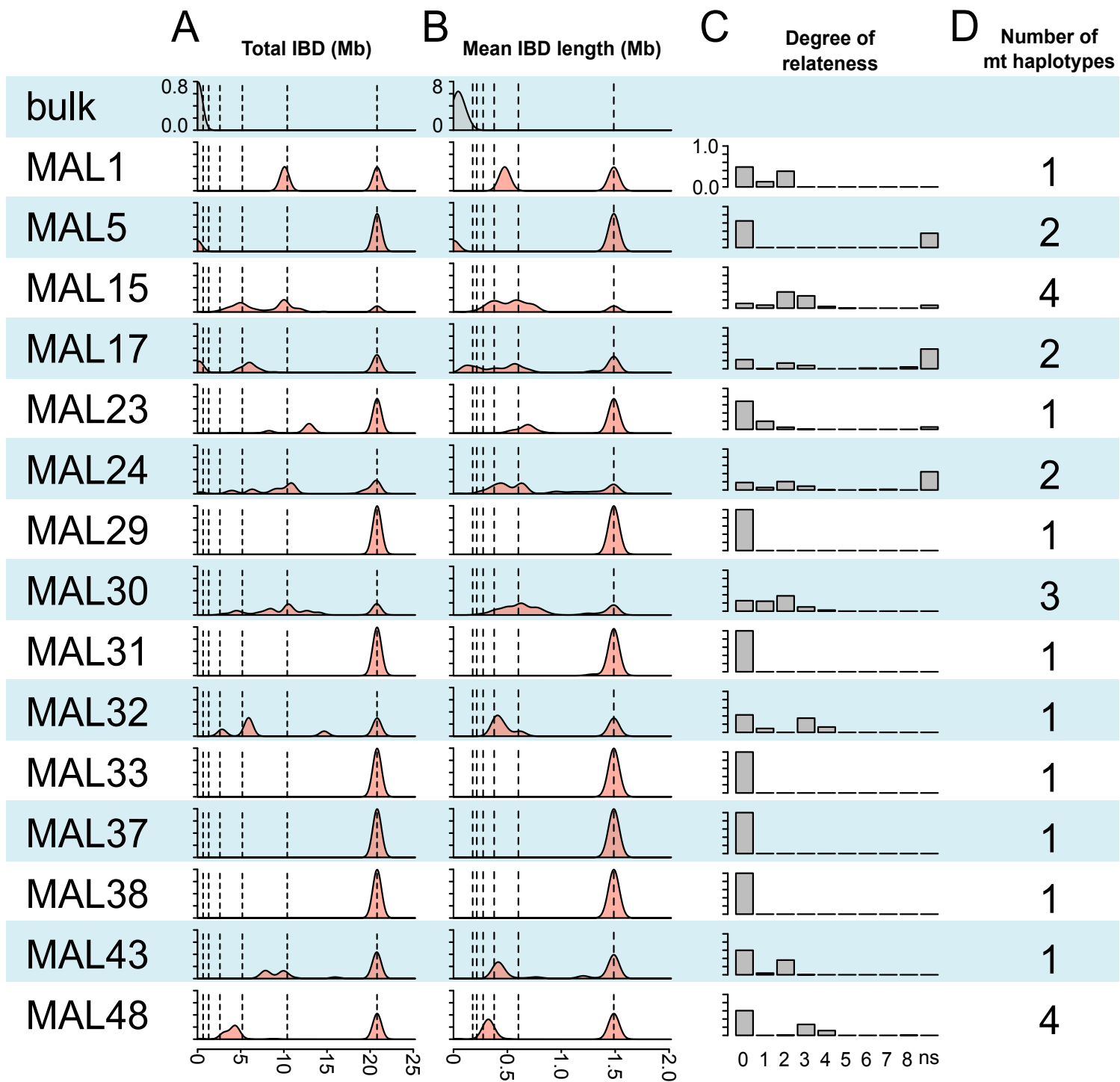
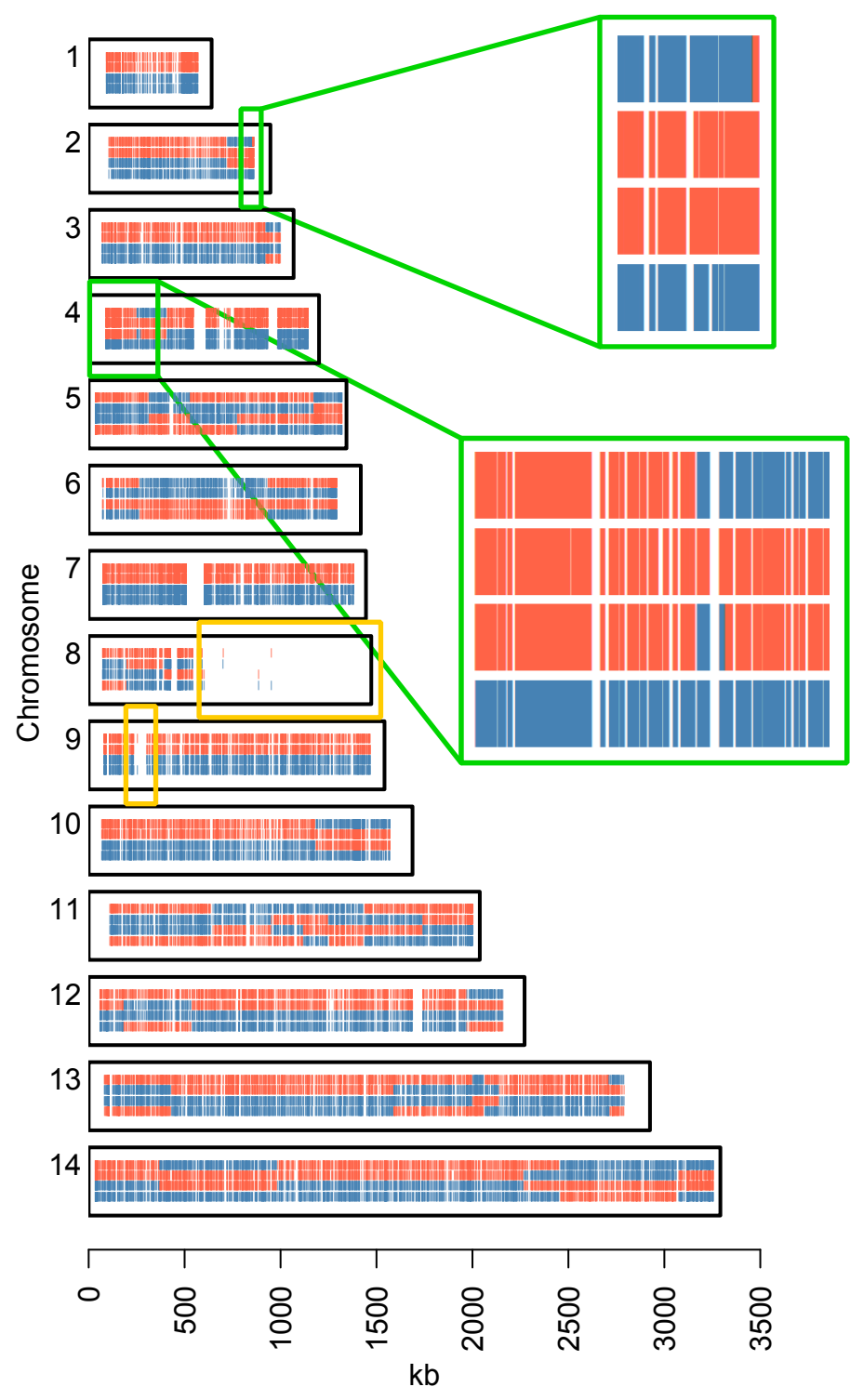


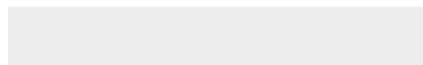
Figure 6





Click here to access/download

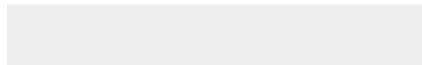
Supplemental Text and Figures
Supplementary_Figures.pdf





[Click here to access/download](#)

Supplemental Videos and Spreadsheets
Supplementary Table 1.xlsx





Click here to access/download

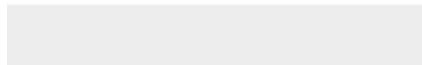
Supplemental Videos and Spreadsheets
Supplementary Data 1.pptx





Click here to access/download

Supplemental Videos and Spreadsheets
Supplementary Data 2.pptx





Click here to access/download

Supplemental Videos and Spreadsheets
Supplementary Data 3.pptx

